The RISE and fall of the Sea

(as seen in satellite altimeter data)

Josef Cherniawsky and Michael Foreman

Institute of Ocean Sciences,Fisheries & Oceans Canada, Sidney, BC

Seminar at the Institute of Ocean Sciences, April 1, 2016

Acknowledgements

Jane Eert, Kerry Kinnersley, Maxim Krassovski (OSD/DFO)

Patrick Cummins, Howard Freeland (OSD/DFO)

Anne Ballantyne, Fred Stephenson (CHS/DFO)

Thomas James, Garry Rogers (PGC/NRCan)

Remko Scharroo (EUMETSAT)

Sok Kuh Kang (KORDI)

Rob Bell (NIWA)

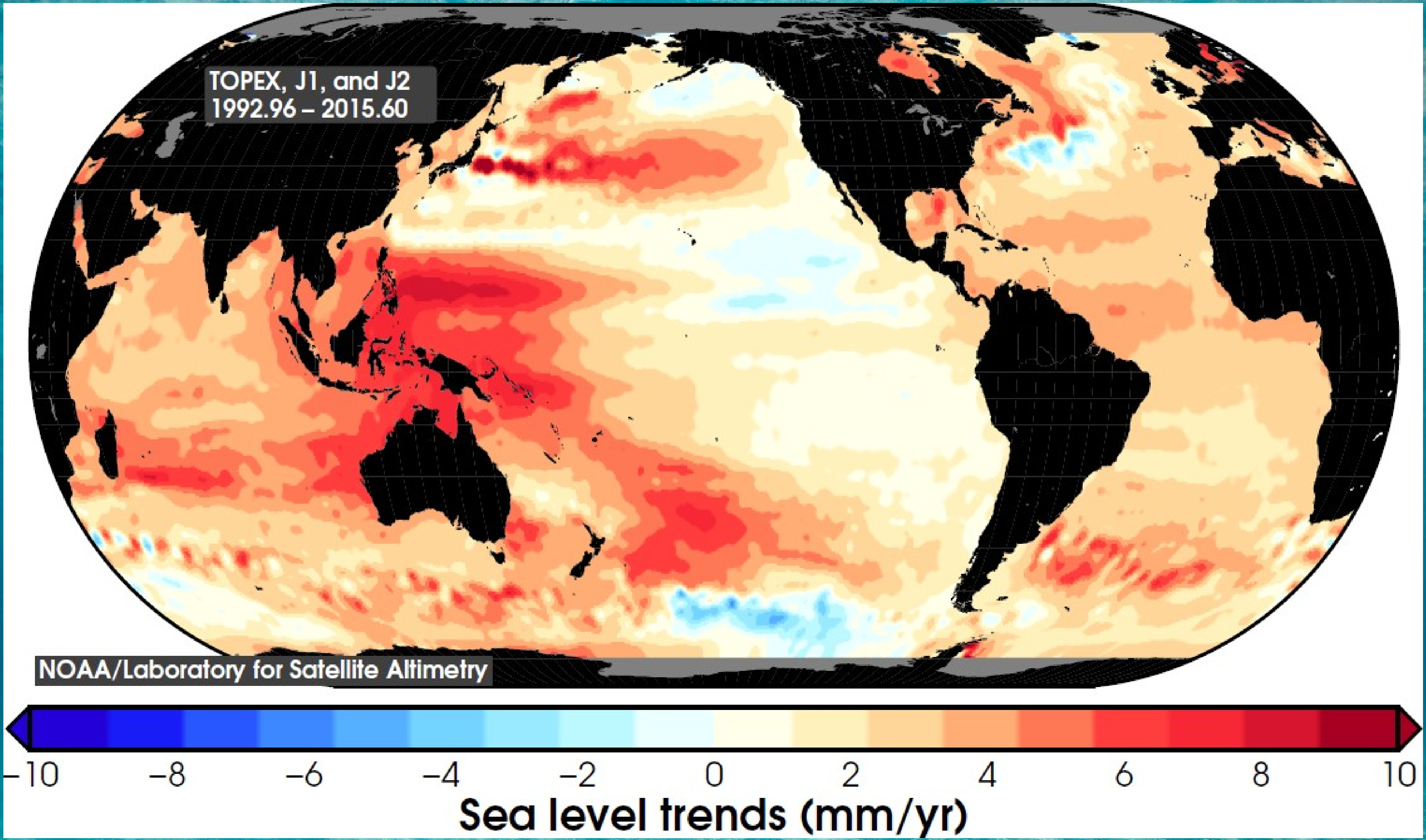
TOPEX, J1, and J2
1992.96 – 2015.60
NOAA/Laboratory for Satellite Altimetry
−10
−8
−6
−4
−2
0
2
4
6
8
10
Sea level trends (mm/yr)

Global mean sea level rise (from NOAA, no GIA applied)

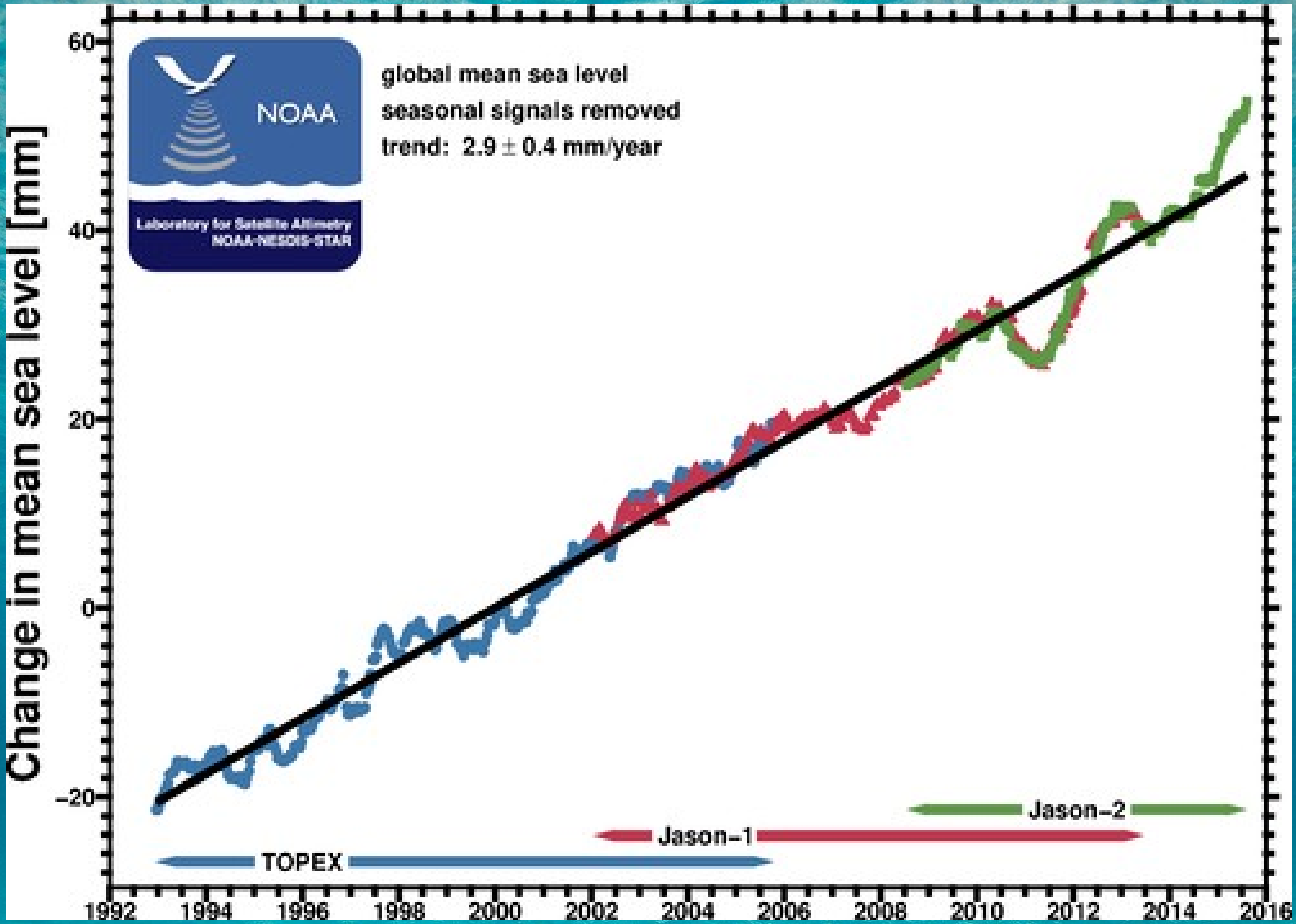

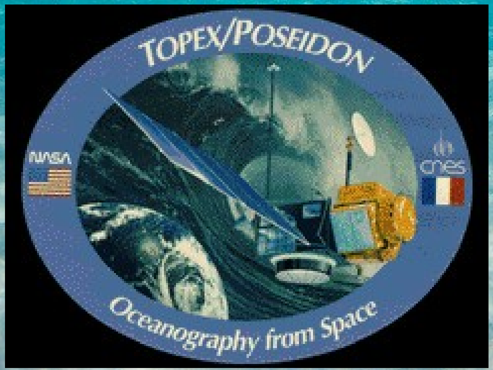

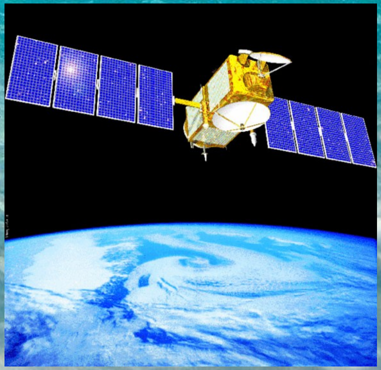

Select regional trends: stronger interannual and decadal variability

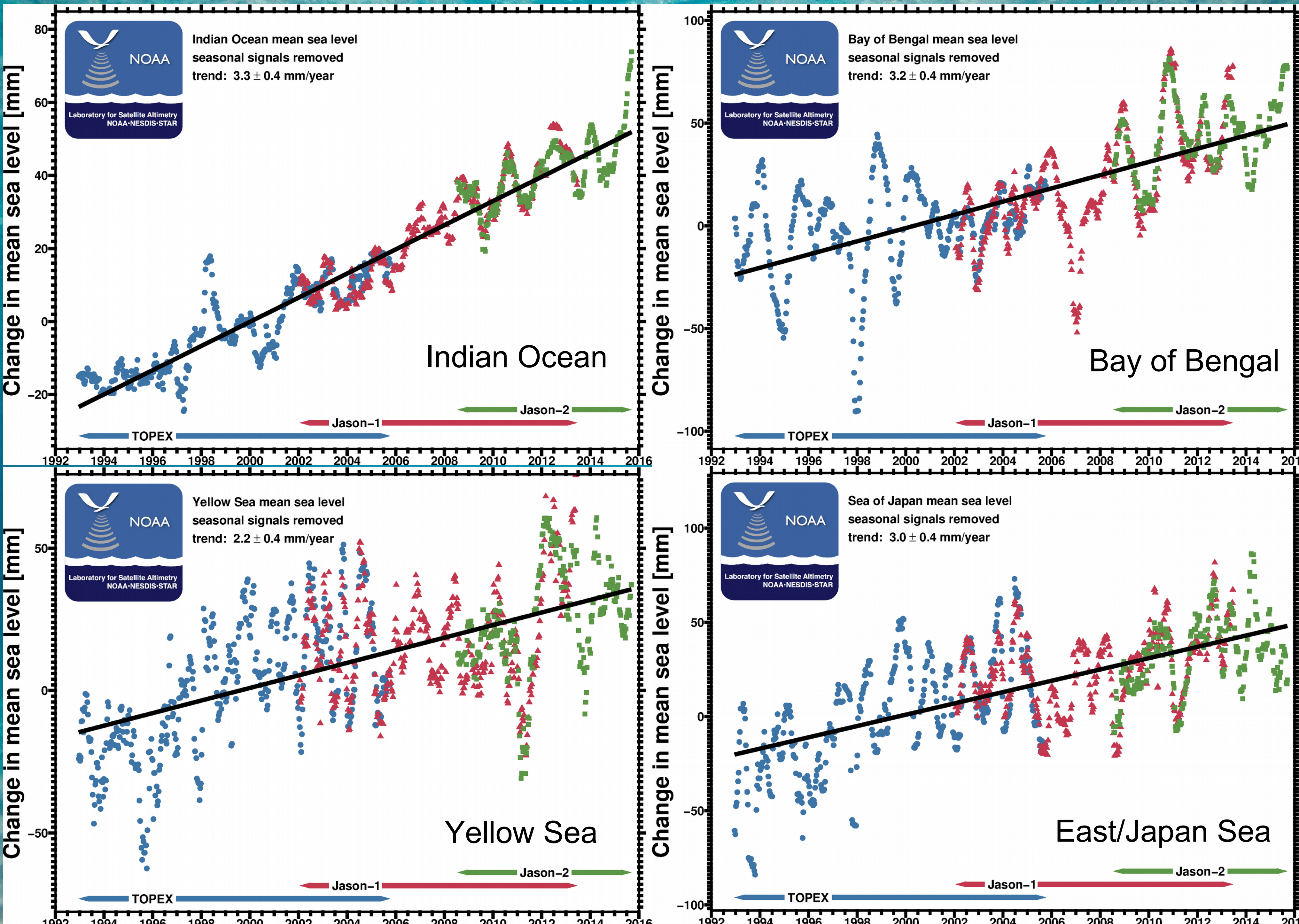

Select regional trends: stronger interannual and decadal variability

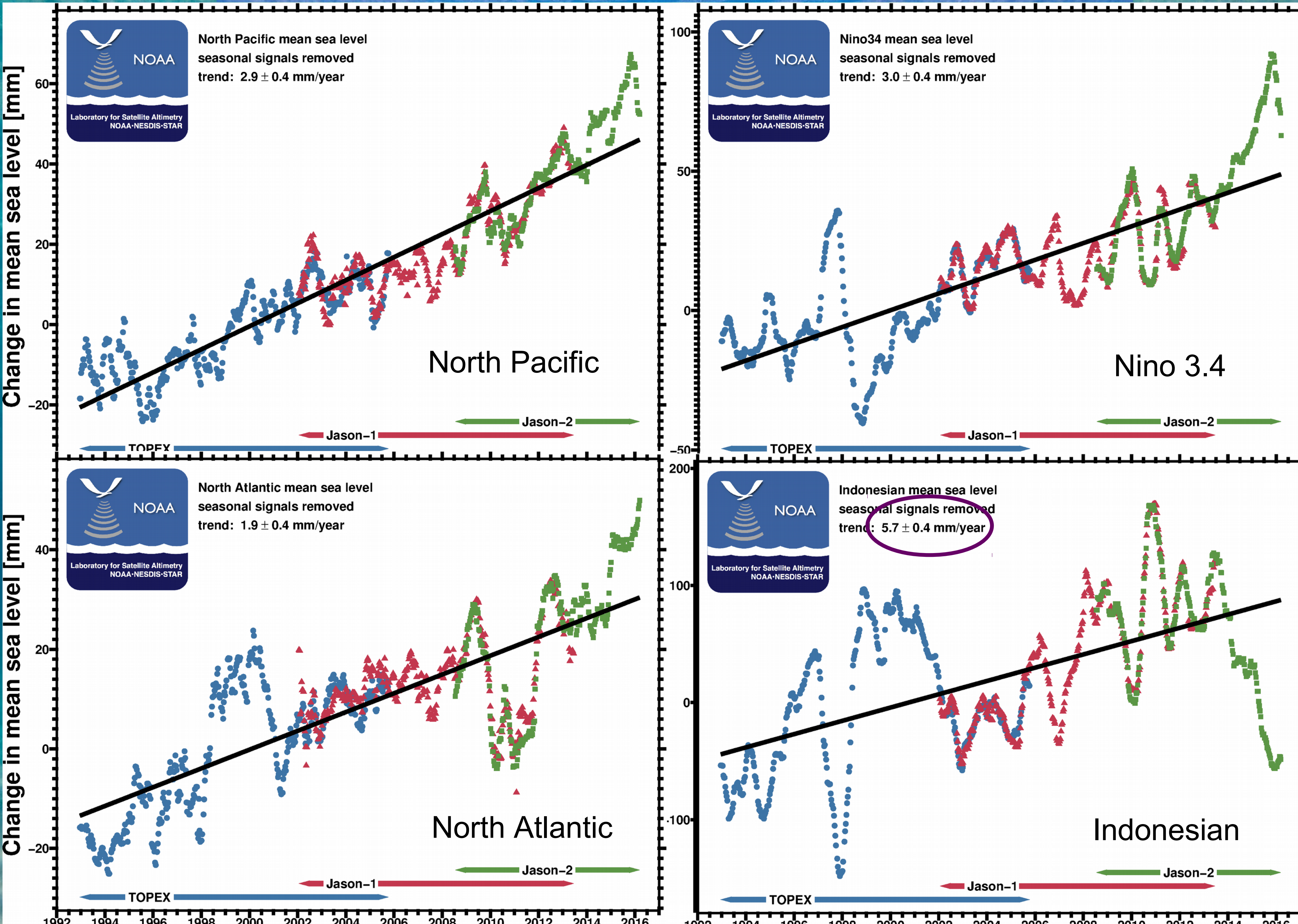

The *aims* of this work are to compute local and regional *sea level trends* from TOPEX/Poseidon, Jason-1 and Jason-2 satellite altimeter data while taking into account the important *modes* of climate variability

We include in the analyzes the following modes/indices:

1. Lunar nodal tide (Mn: period = 18.6 years)
2. Low-pass filtered Pacific Decadal Oscillation (PDO) Index
3. High-pass filtered Multivariate ENSO Index (MEI)

The IOS Versatile Analysis (IVA)

we modify the **Versatile Harmonic Analysis** (Foreman et al. 2009)

$$h(t_j) = Z_0 + \boxed{a}(t_j - t_c) + \sum_{k=1}^{n} f_k(t_j) A_k \cos\left[V_k(t_j) + u_k(t_j) - g_k\right] + R(t_j)$$

Trend

to also include non-harmonic climate indices

$$h(t_j) = Z_0 + \boxed{a}(t_j - t_c) + \boxed{\sum_{i=1}^{N_C} b_i I_i(t_j)} + \sum_{k=1}^{n} f_k(t_j) A_k \cos\left[V_k(t_j) + u_k(t_j) - g_k\right] + R(t_j)$$

N_c = number of climate indices (I_i) and n = number of harmonic terms

We use SVD to solve for Z_0, a, b_i $(i=1,N_c)$, A_k and g_k $(k=1,n)$

with corresponding *constituent error covariances* and *correlations:*

$$\boxed{r_{ij} = C_{ij} / \sqrt{(C_{ii} C_{jj})}}$$

(*Cherniawsky et al.* 2001, 2010; *Foreman et al.* 2009)

But ENSO (MEI) and PDO are not independent!

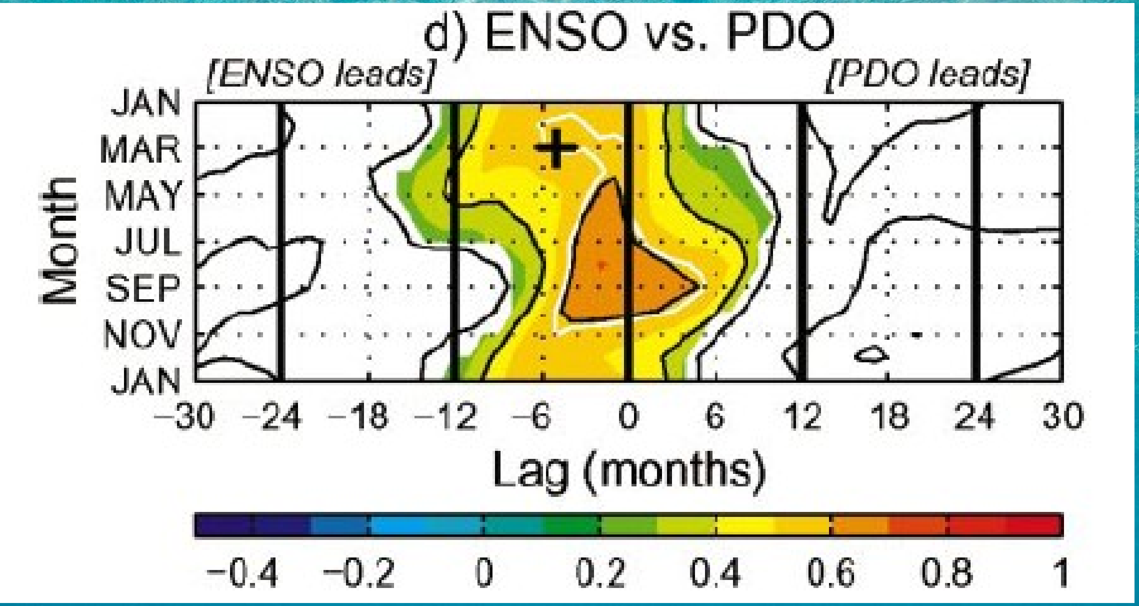

(from Newman et al., *J. Climate* 2003)

Therefore, when we use MEI and PDO indices ‘as is’ their analysed amplitudes are correlated, with r~0.5! We therefore choose to filter these indices.

Input: Unfiltered & Low-Pass Filtered PDO Index

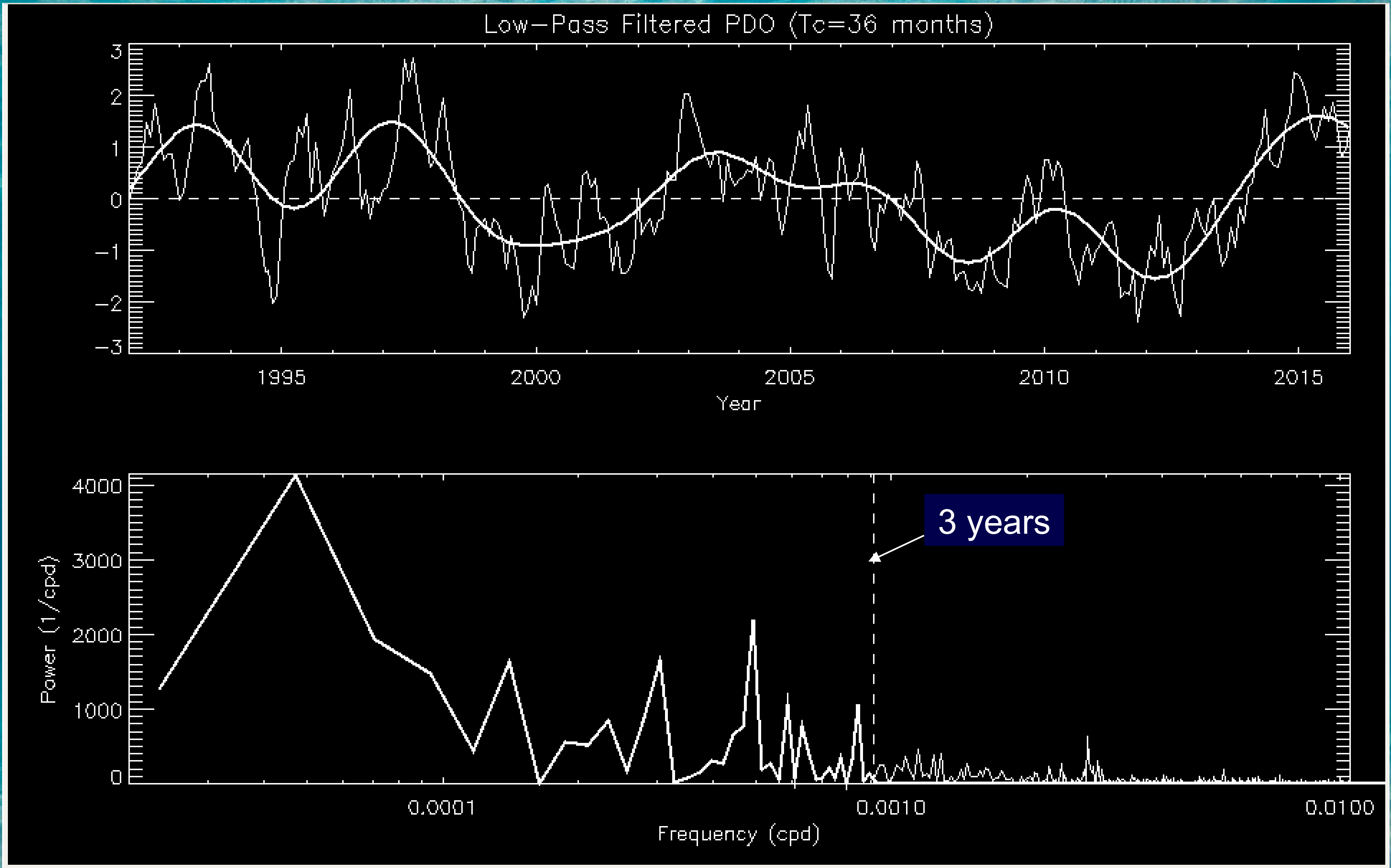

Input: Unfiltered & High-Pass Filtered MEI

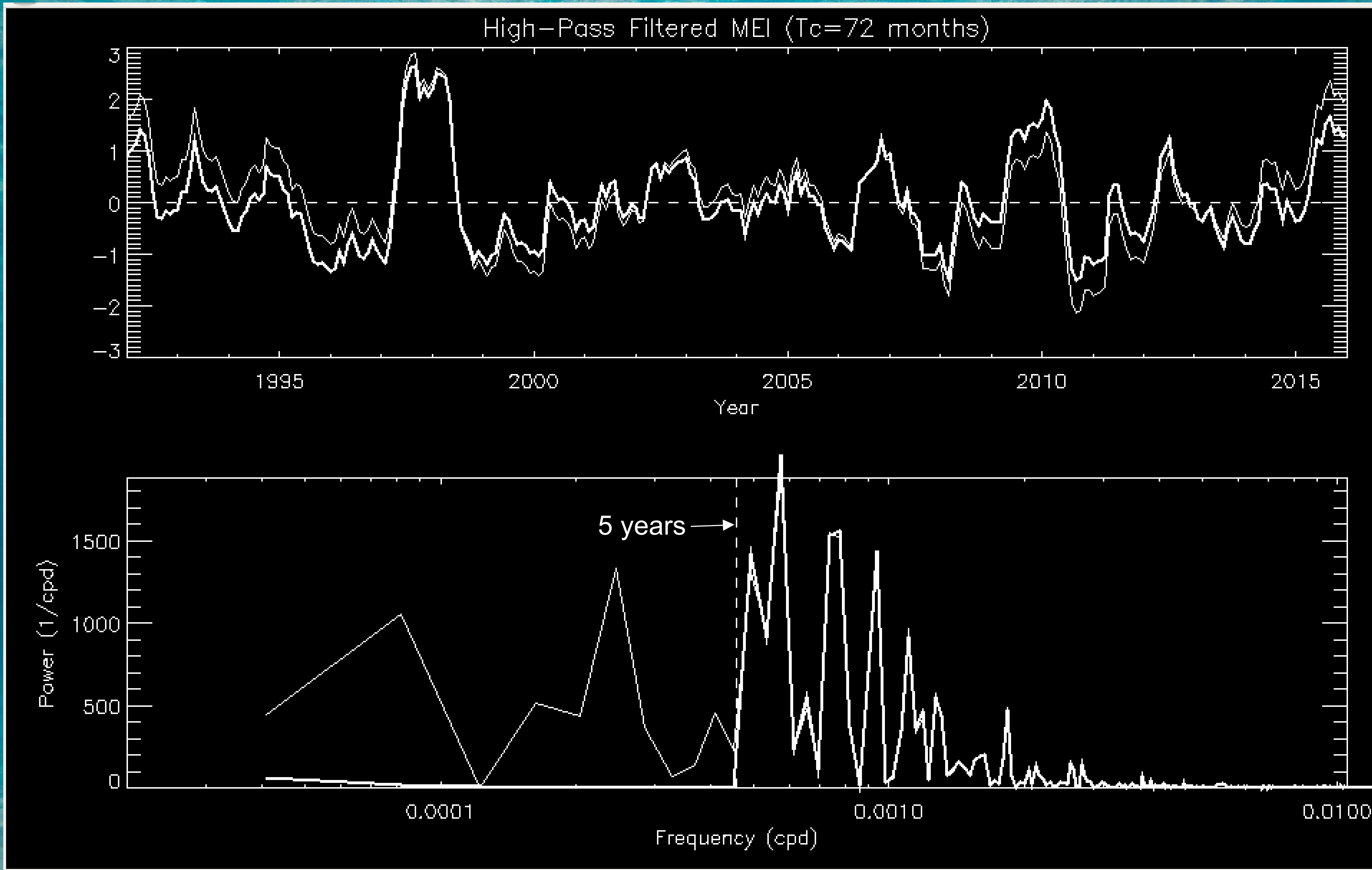

Trend is computed

```
31 1 1
     Z0          0.0000000000
     PDO         0.0000000000   PDO index
     MEI         0.0000000000   MEI index
     Mn          0.0000061290   18.6-yr
     SA          0.0001140741
     SSA         0.0002281591
     MM          0.0015121518
     MF          0.0030500918
     Q1n         0.0372123736   nodal sat
     Q1          0.0372185026
     RHO1        0.0374208736
     O1n         0.0387245256   nodal sat
     O1          0.0387306544
     NO1         0.0402685944
     P1          0.0415525871
     S1          0.0416666721
     K1          0.0417807462
     K1n         0.0417868751   nodal sat
     PSI1        0.0418948203
     J1          0.0432928981
     2N2         0.0774870970
     MU2         0.0776894680
     N2          0.0789992488
     NU2         0.0792016198
     M2n         0.0805052717   nodal sat
     M2          0.0805114007
     L2          0.0820235525
     T2          0.0832192592
     S2          0.0833333333
     K2          0.0835614924
     K2n         0.0835676239   nodal sat
    23    09    92    28    01    16    19    20
```

An example of the IVA list of constituents (*tide14_rv.dat*)

Analysis results at a single TPJ location off Vancouver Island (48.89N, 126.01W)

		AMPLITUDE	PHASE LAG	Amp SD Est.	t-test value
Z0	0.000000000	-0.01180	0.000	0.00383	3.08
Trend	0.000000000	0.00168	0.000	0.00159	1.06
PDO	0.000000000	0.02194	0.000	0.00486	4.51
MEI	0.000000000	0.01881	0.000	0.00701	2.68
Mn	0.000006129	0.00876	342.579	0.00732	1.20
SA	0.000114074	0.08616	2.380	0.00741	11.63
SSA	0.000228159	0.02210	237.800	0.00668	3.31
MM	0.001512152	0.00587	171.076	0.00616	0.95
MF	0.003050092	0.01513	170.605	0.00622	2.43
Q1n	0.037212372	0.00540	279.916	0.00663	0.81
Q1	0.037218504	0.04454	216.482	0.00689	6.47
RHO1	0.037420873	0.00227	261.364	0.00612	0.37
O1n	0.038724527	0.05064	226.418	0.00624	8.11
O1	0.038730655	0.25623	226.516	0.00670	38.24
NO1	0.040268596	0.01620	240.833	0.00576	2.81
P1	0.041552588	0.12720	235.380	0.00679	18.73
S1	0.041666672	0.01374	244.933	0.00904	1.52
K1	0.041780747	0.42079	240.437	0.00675	62.30
K1n	0.041786876	0.04631	248.442	0.00714	6.49
PSI1	0.041894820	0.00269	313.953	0.00661	0.41
J1	0.043292899	0.01961	233.485	0.00628	3.12
2N2	0.077487096	0.02004	186.094	0.00630	3.18
MU2	0.077689469	0.02215	181.148	0.00623	3.56
N2	0.078999251	0.19707	210.660	0.00650	30.30
NU2	0.079201616	0.04013	209.014	0.00632	6.35
M2n	0.080505274	0.04017	232.857	0.00638	6.29
M2	0.080511399	0.95505	236.550	0.00679	140.57
L2	0.082023554	0.02026	248.364	0.00631	3.21
T2	0.083219260	0.01922	247.112	0.00638	3.01
S2	0.083333336	0.27314	264.767	0.00638	42.79
K2	0.083561495	0.06720	255.493	0.00680	9.89
K2n	0.083567627	0.02202	250.436	0.00690	3.19

```
1 largest correlation coef. =  0.2936 at (i,j)=   6    2 for Mn    and Trend
2 largest correlation coef. =  0.2834 at (i,j)=   4    3 for MEI   and PDO
3 largest correlation coef. =  0.2427 at (i,j)=   5    3 for Mn    and PDO
4 largest correlation coef. =  0.2034 at (i,j)=   3    2 for PDO   and Trend
5 largest correlation coef. =  0.1847 at (i,j)=   7    4 for SA    and MEI
6 largest correlation coef. =  0.1729 at (i,j)=   6    5 for Mn    and Mn
7 largest correlation coef. =  0.1506 at (i,j)=   5    2 for Mn    and Trend
8 largest correlation coef. =  0.1404 at (i,j)=  18   15 for Q1    and Q1n
```

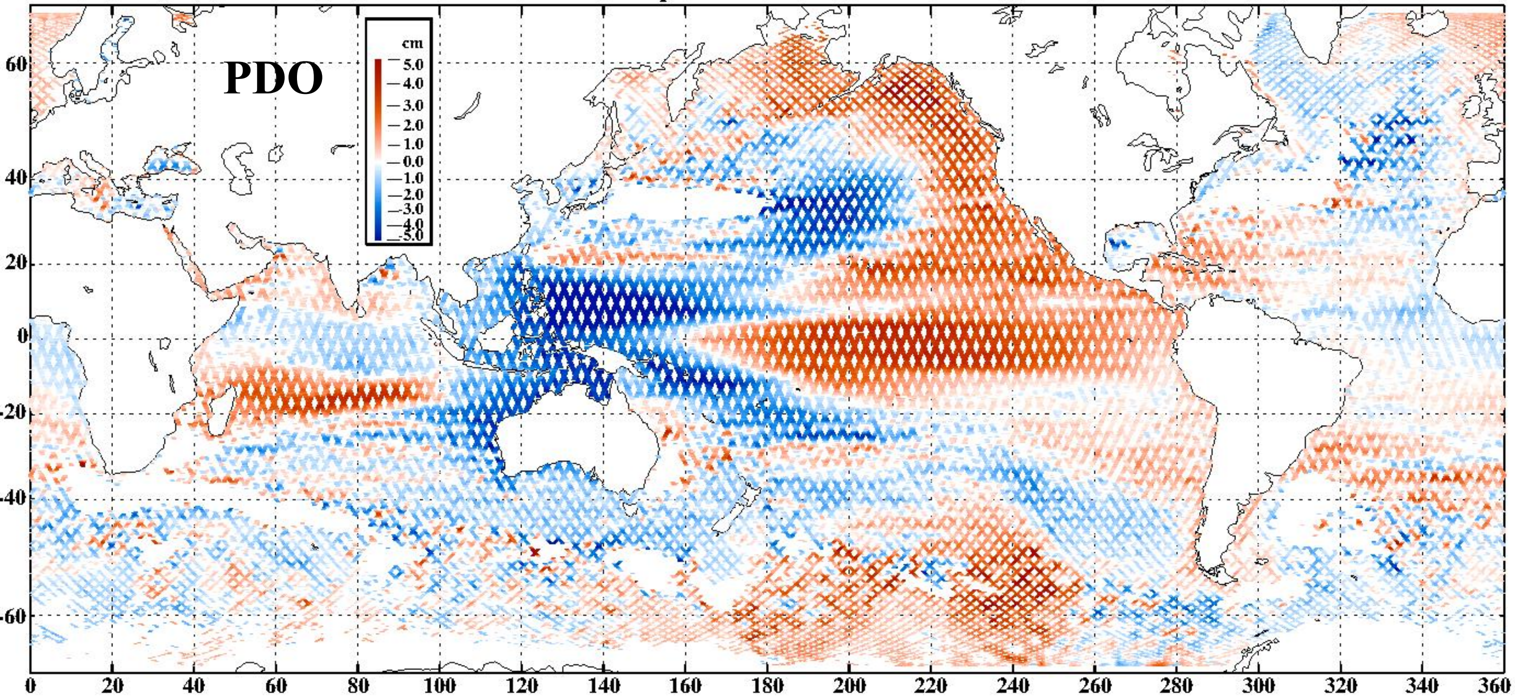

Min, Max, Mean, StDev: -10.56, 10.09, 0.05, 1.95 cm (N=351534) Mean sig = 0.45 cm (trk..._rrv.out.bin)

(excluded 187175 locations with ampl < sigma, 111 near Xs [redit=0.5] and 17150 locations with rms residual > 15 cm)

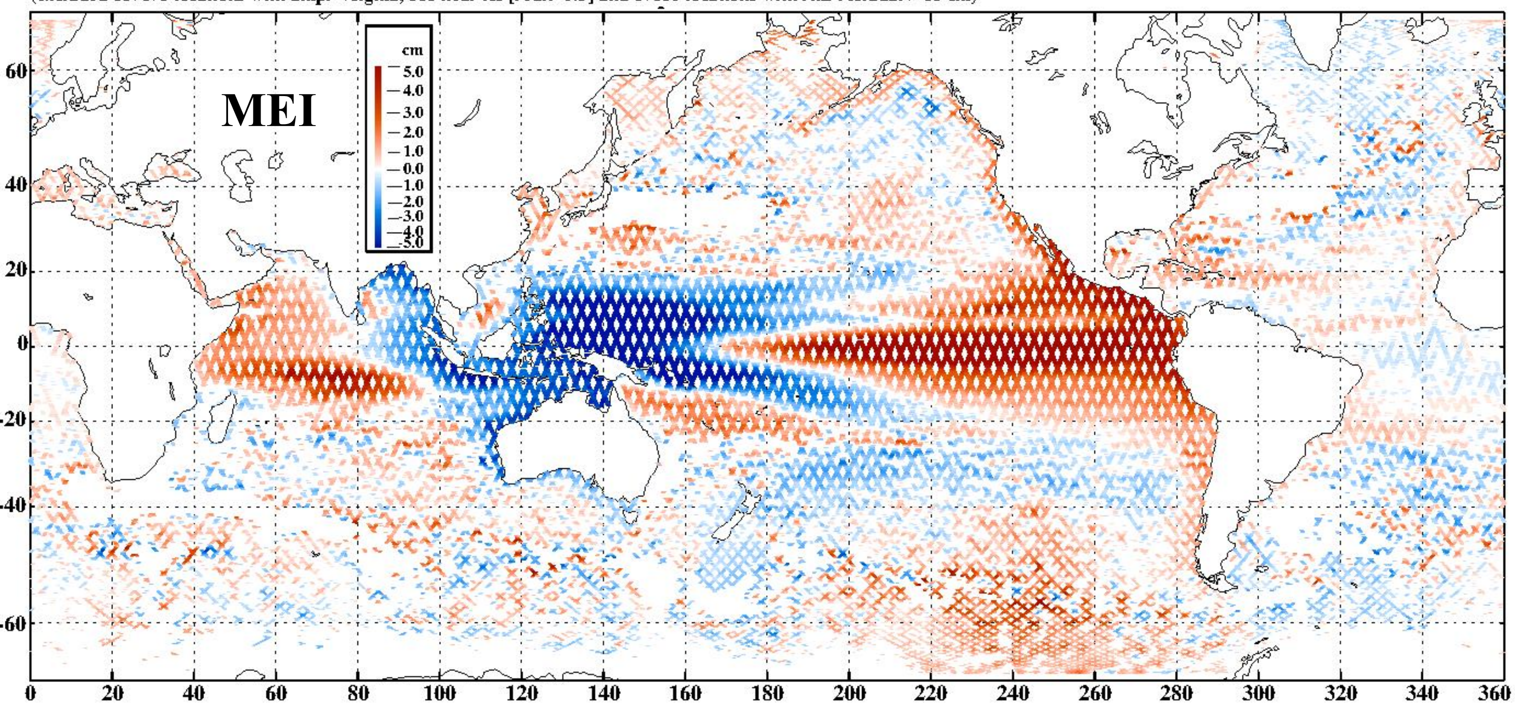

Min, Max, Mean, StDev: -9.54, 8.08, 0.33, 2.31 cm (N=258275) Mean sig = 0.62 cm (trk..._rrv.out.bin)

(excluded 287439 locations with ampl < sigma and 10256 locations with rms residual > 15 cm)

Theoretical Amplitude of the 18.6-year Lunar Nodal Tide

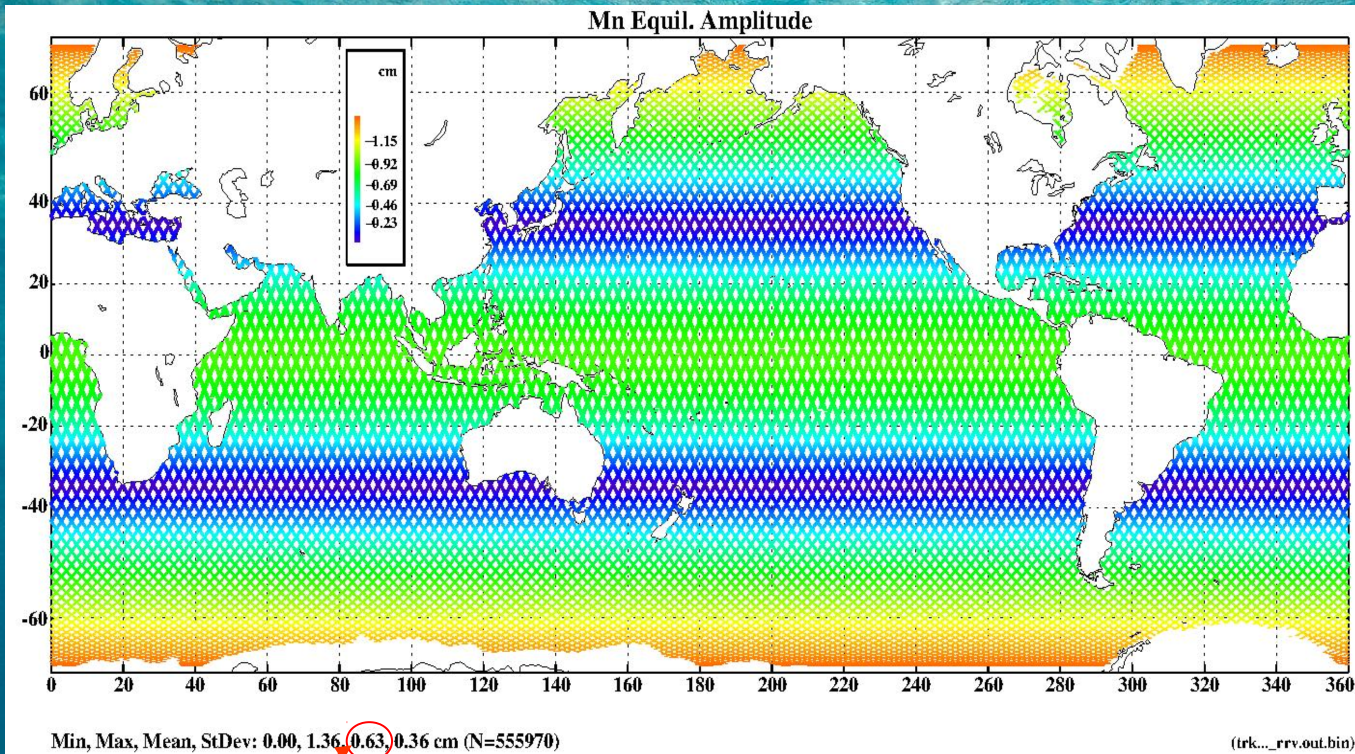

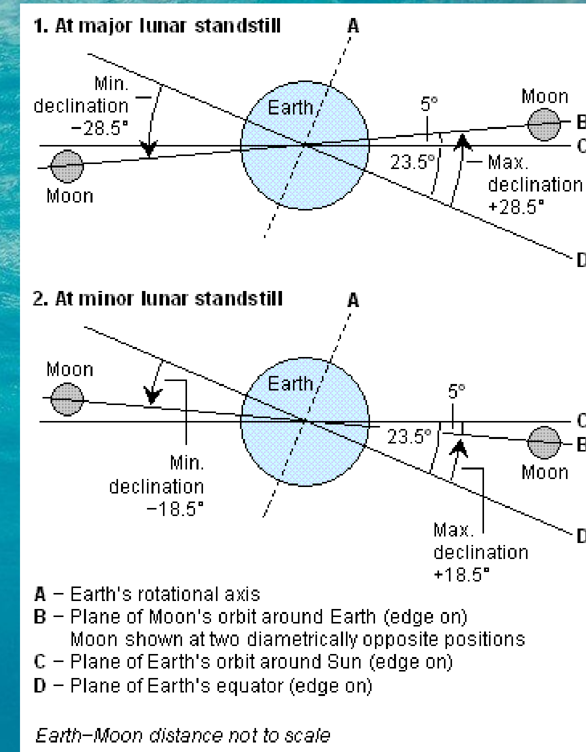

Mean = 0.63 cm

$$H_N = 18\left(\tfrac{3}{2}\sin^2\varphi - \tfrac{1}{2}\right)\cos N \quad \text{(in mm)}$$

N is the mean longitude of the Moon's ascending node
Last maximum of cos N (when N=0) was in Nov. 2006

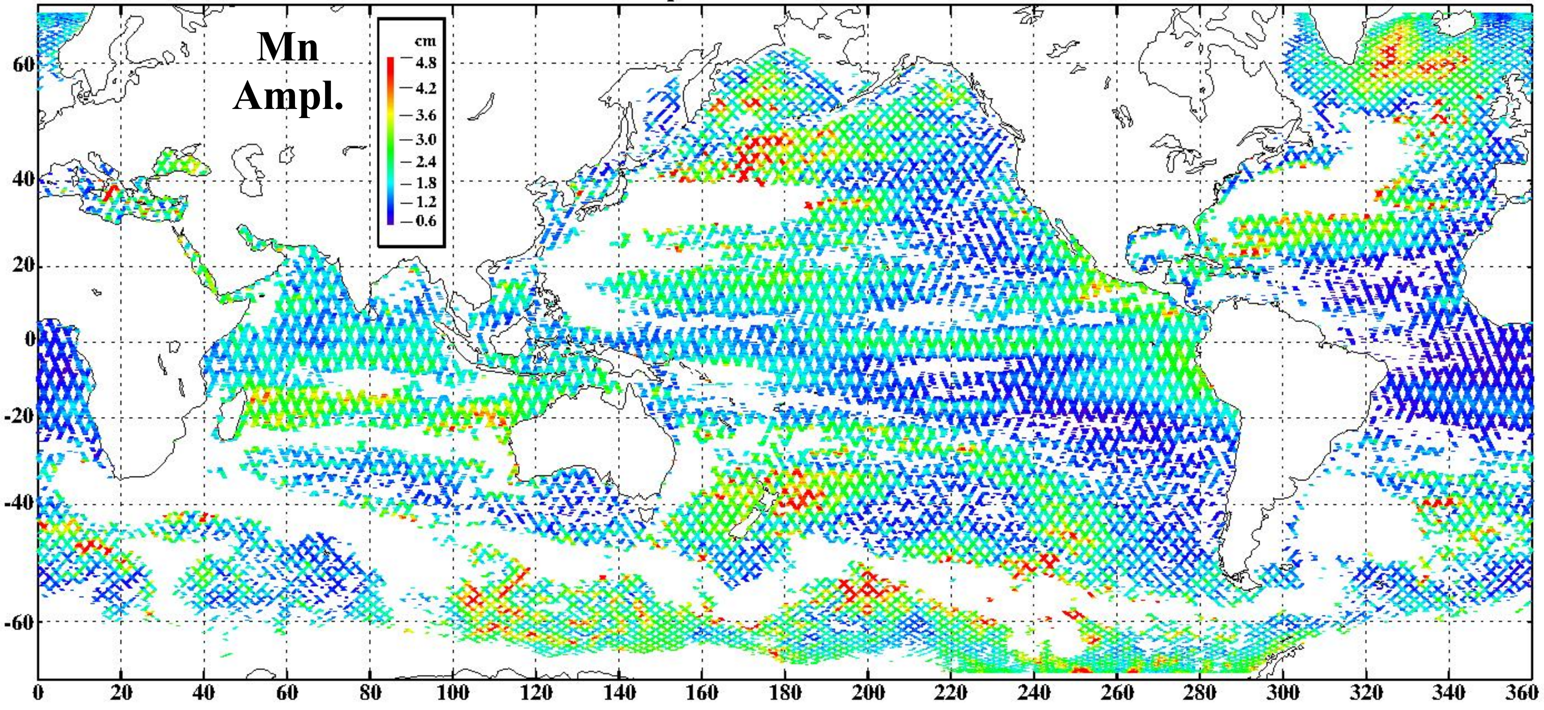

Min, Max, Mean, StDev: 0.55, 11.23, 2.00, 0.87 cm (N=291834) Mean sig = 0.56 cm (trk..._rrv.out.bin)
(excluded 208337 locations with r < 2.0, 118 near Xs [redit=0.5] and 55681 locations with rms residual > 10 cm)

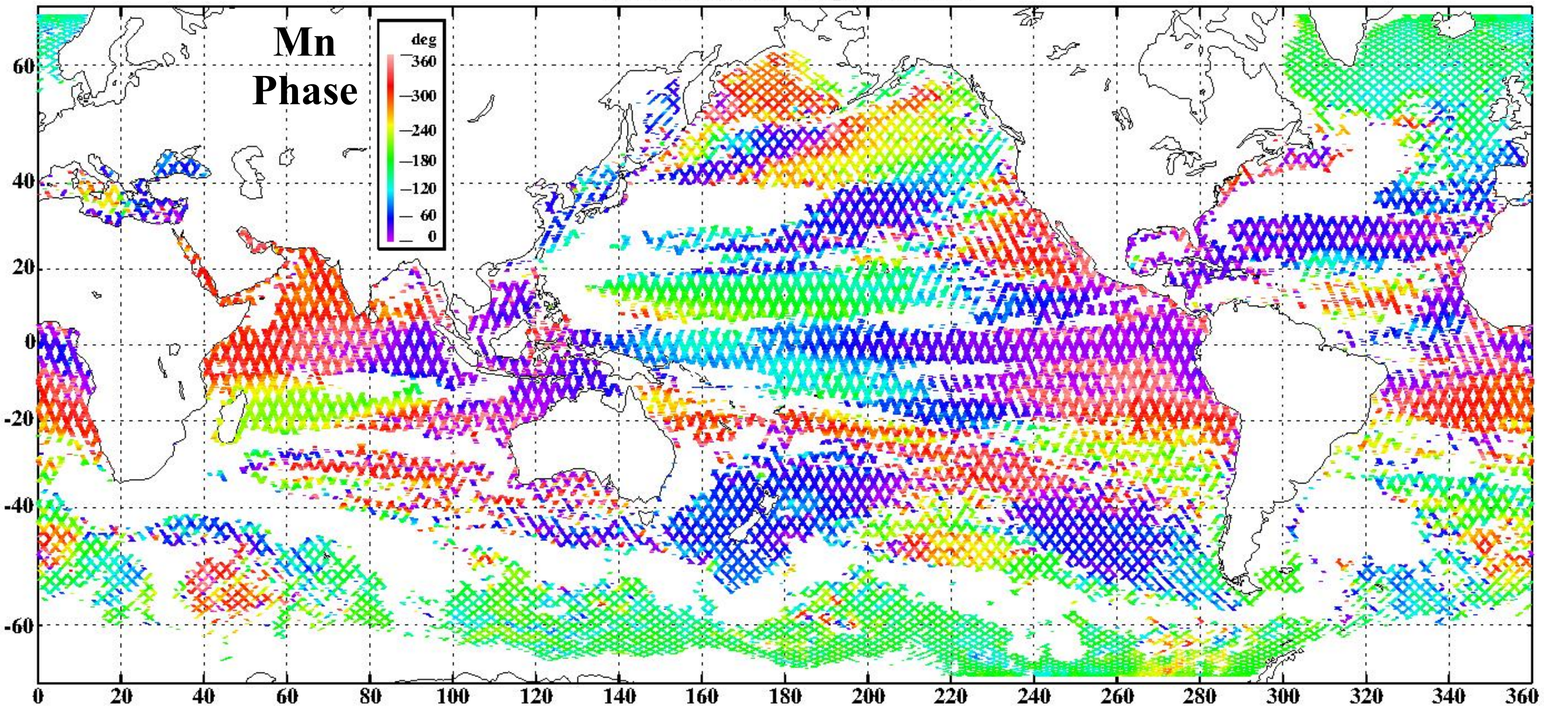

Min, Max, Mean, StDev: 0.0, 359.0, 163.8, 110.3 deg (N=291834) Mean sig = 0.56 cm (trk..._rrv.out.bin)

Analyzed 18.6-year lunar nodal tide (Mn)

Mean amplitude is 2.0 cm, i.e. ~3 times larger than theoretical

Mn phase & amplitude have strong regional variations

and

do not look at all like the theoretical Mn!

Lunar nodal satellites

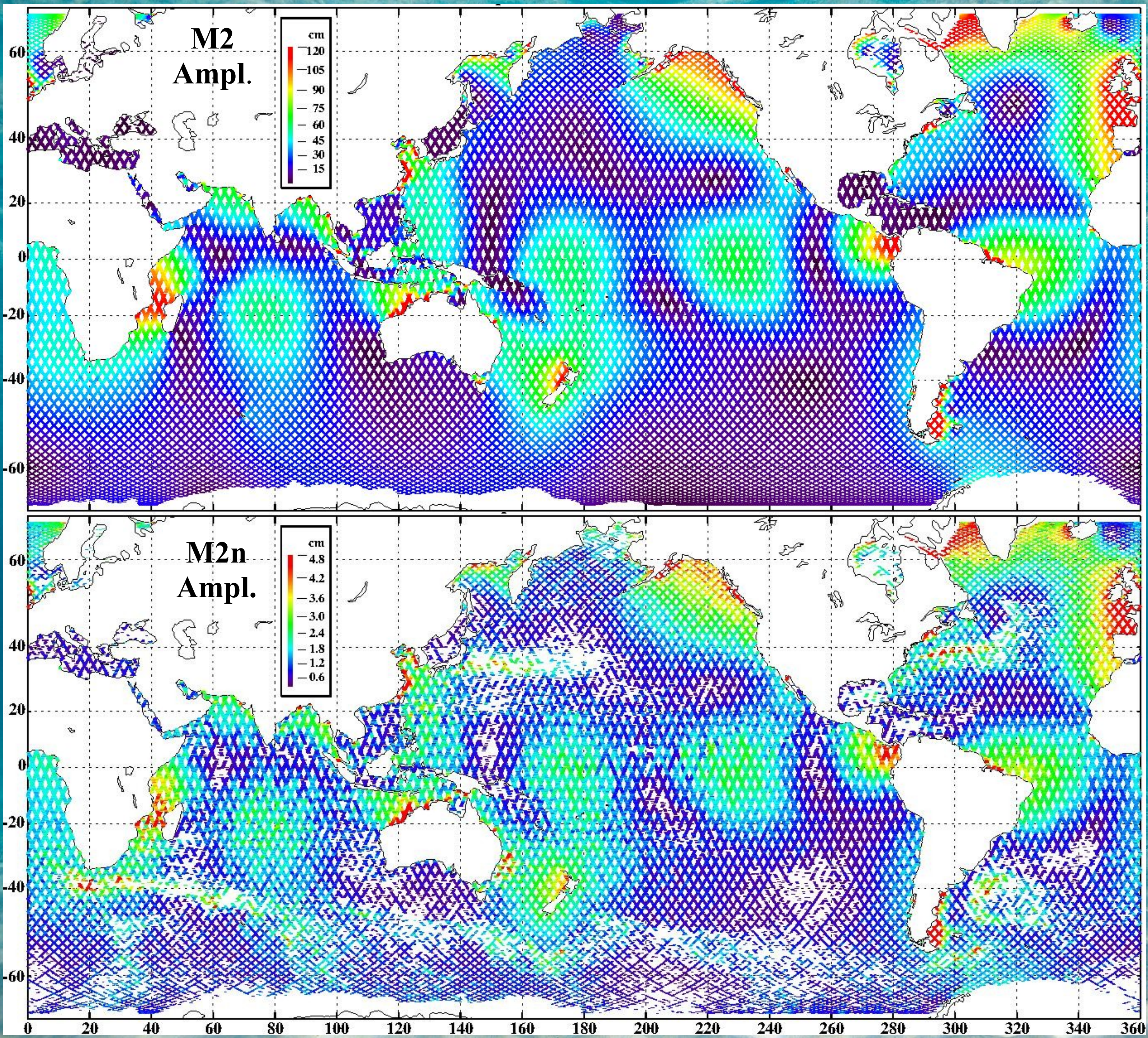

Analyzed M2 & M2n amplitudes

Note the different amplitude scales!

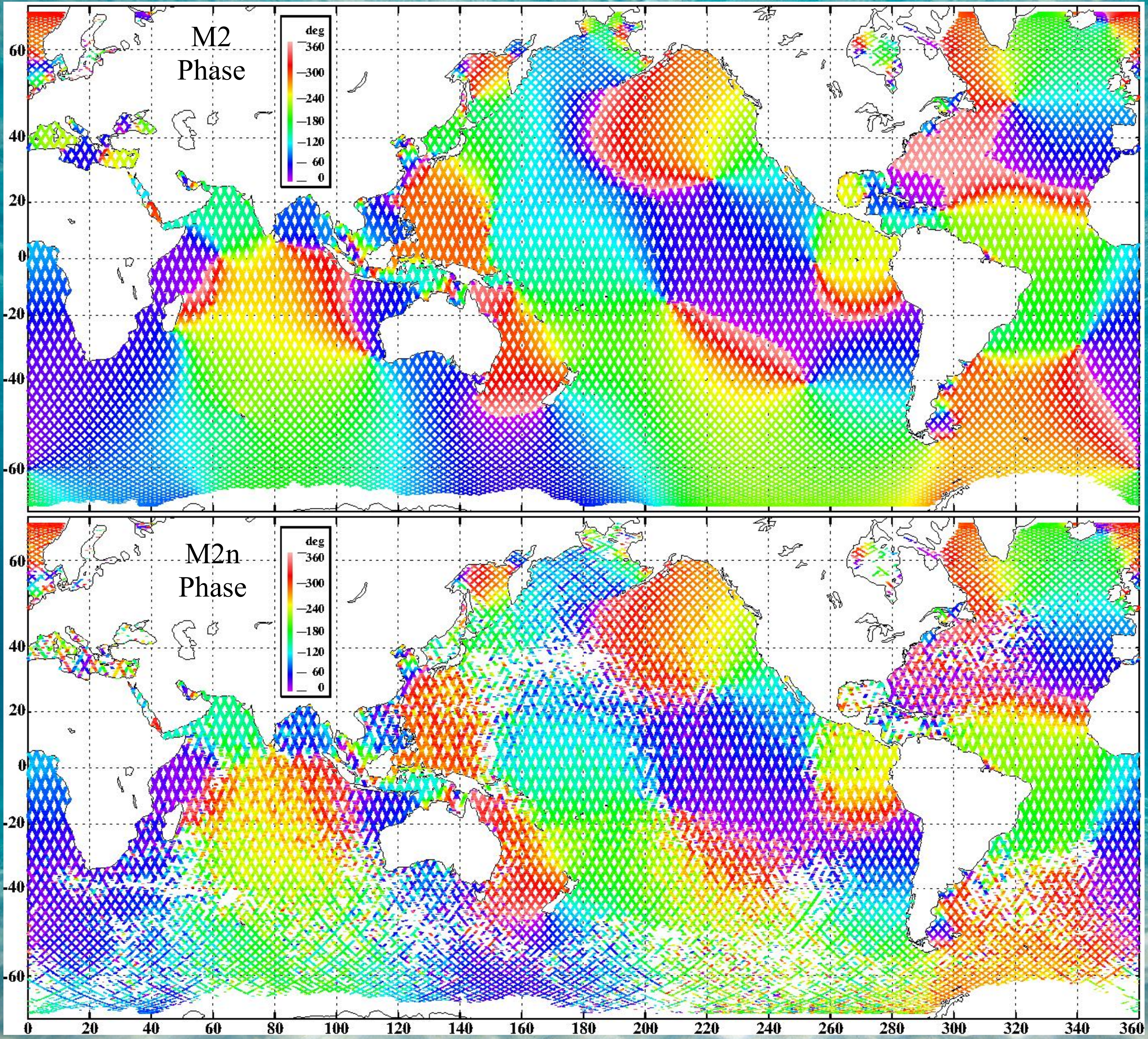

Analyzed M2 & M2n phases:

They are in phase!

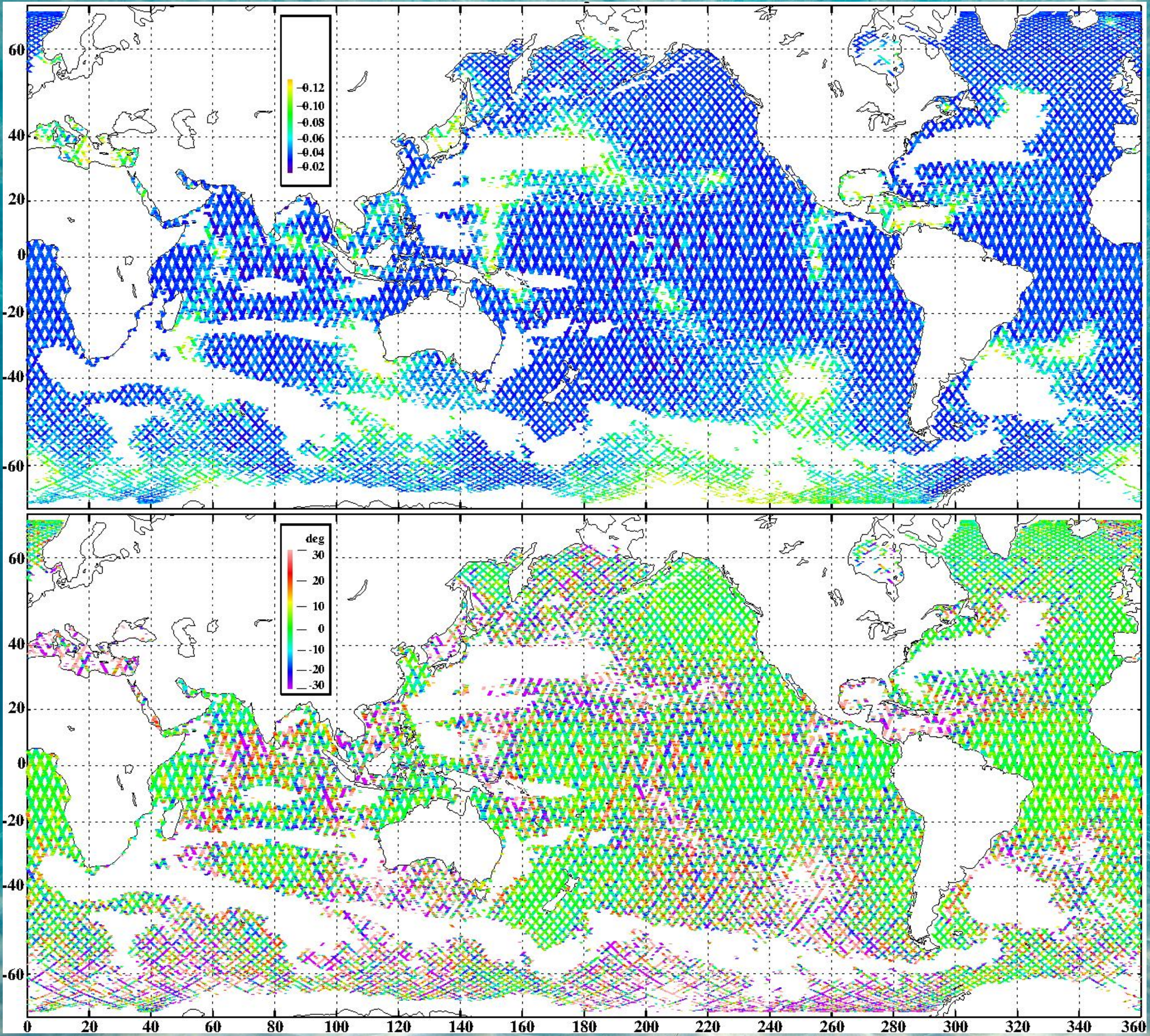

<u>M2n/M2 amplitude ratio</u>

median: 4.0%

theory: 3.7%

<u>M2n-M2 phase difference</u>

median: 0.9 deg

theory: 0.0 deg

(see also Cherniawsky et al., *Cont. Shelf Res*. 2010)

A conclusion: the 18.6-year 'tide' is generated from modulation of the diurnal and semi-diurnal tides by lunar nodal satellites

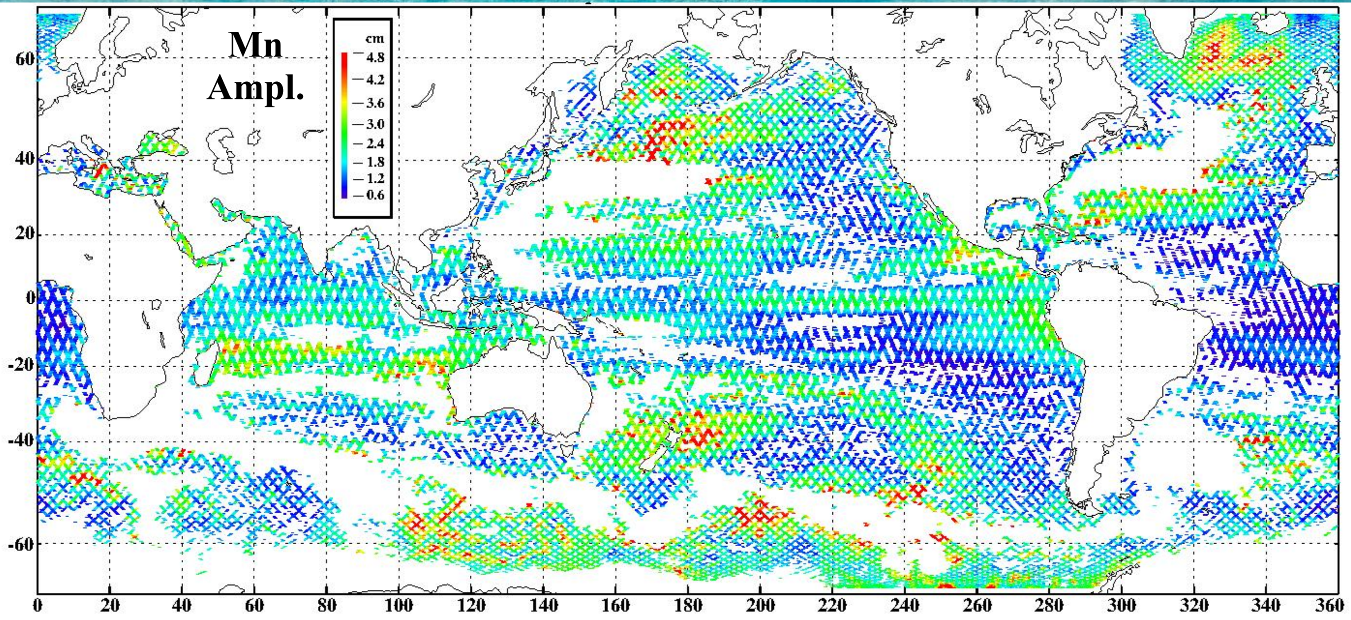

Min, Max, Mean, StDev: 0.55, 11.23, 2.00, 0.87 cm (N=291834) Mean sig = 0.56 cm (trk..._rrv.out.bin)
(excluded 208337 locations with r < 2.0, 118 near Xs [redit=0.5] and 55681 locations with rms residual > 10 cm)

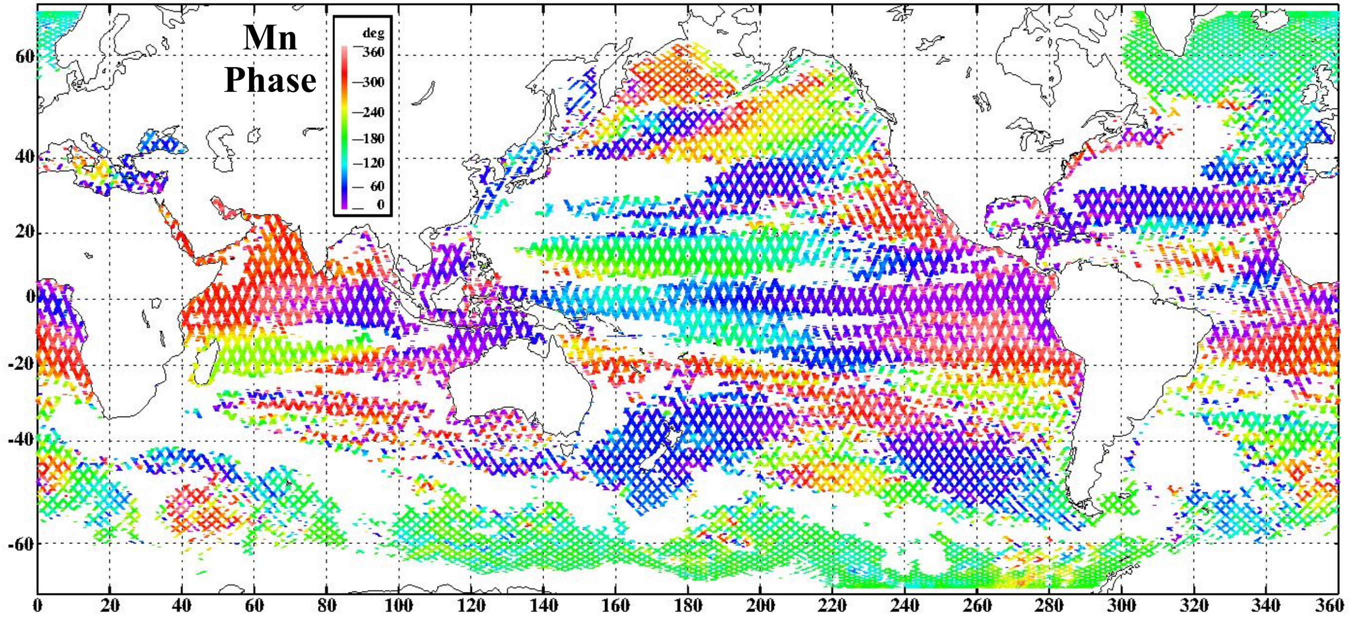

Min, Max, Mean, StDev: 0.0, 359.0, 163.8, 110.3 deg (N=291834) Mean sig = 0.56 cm (trk..._rrv.out.bin)

(for 18.6-year tide in Bering Sea, see Foreman et al., *J. Mar. Res*. 2006)

Analyzes results: Linear Trend (Sep. 1992 to Jan. 2016)

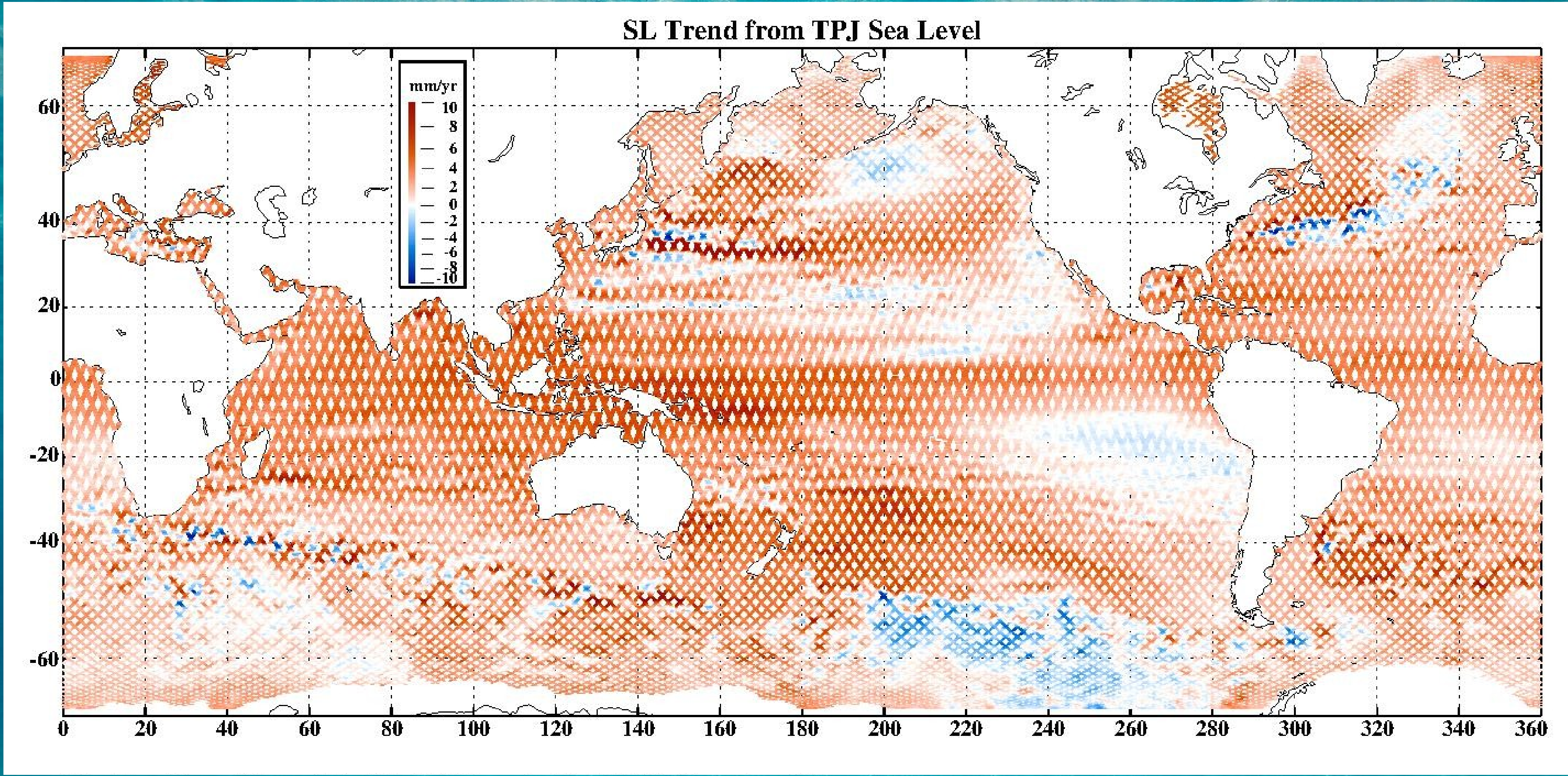

Average trend = 2.8 mm/yr (without GIA)
Its average error = 1.25 mm/yr
(N=555,970 TPJ locations)

We repeated these analyzes at TPJ pass cross-overs
and inspect the effects of climate indices on
sea level trends at select cross-over locations

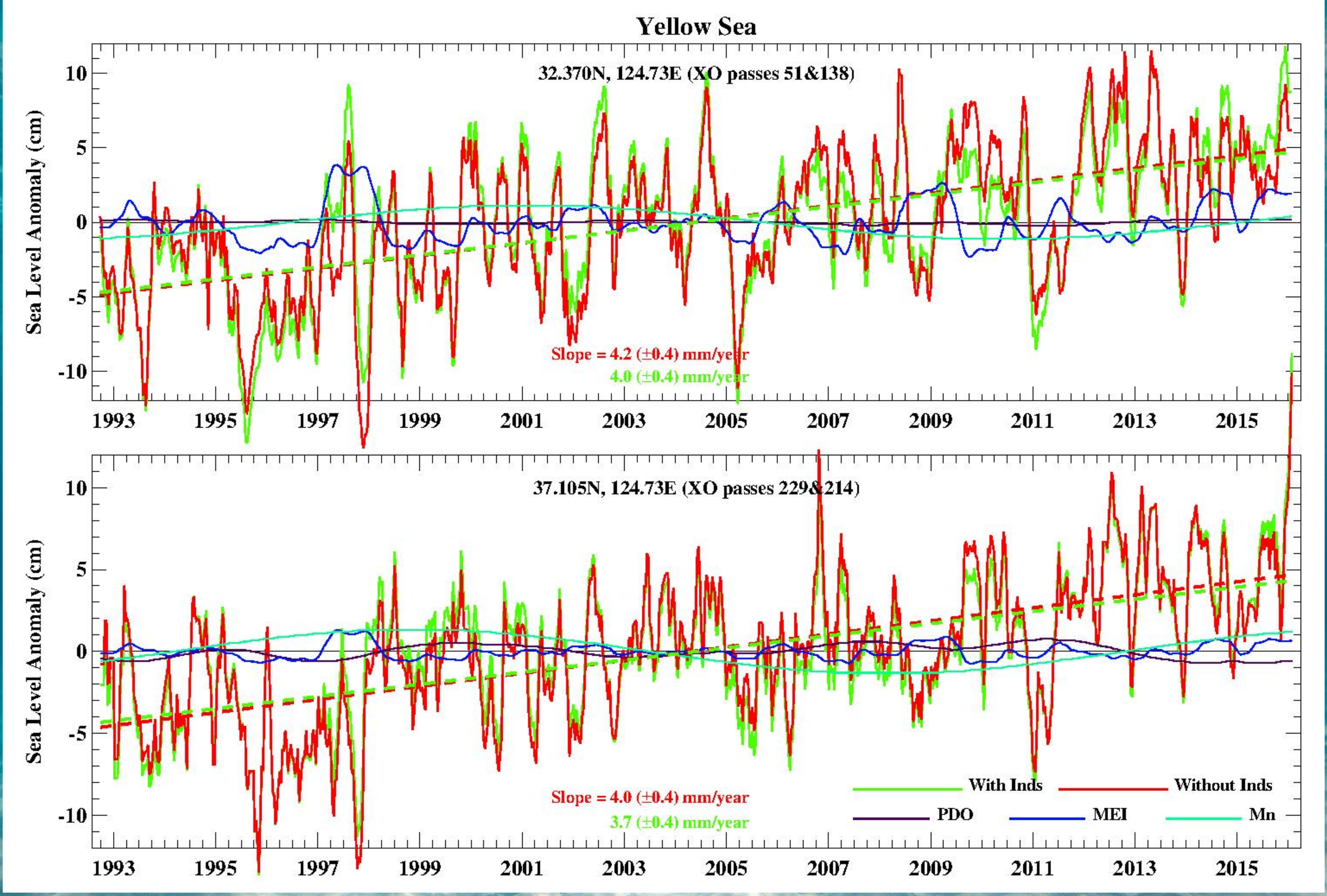

Yellow Sea
32.370N, 124.73E (XO passes 51&138)
Slope = 4.2 (±0.4) mm/year
4.0 (±0.4) mm/year
37.105N, 124.73E (XO passes 229&214)
Slope = 4.0 (±0.4) mm/year
3.7 (±0.4) mm/year
With Inds
Without Inds
PDO
MEI
Mn
Sea Level Anomaly (cm)
10
5
0
-5
-10
1993
1995
1997
1999
2001
2003
2005
2007
2009
2011
2013
2015

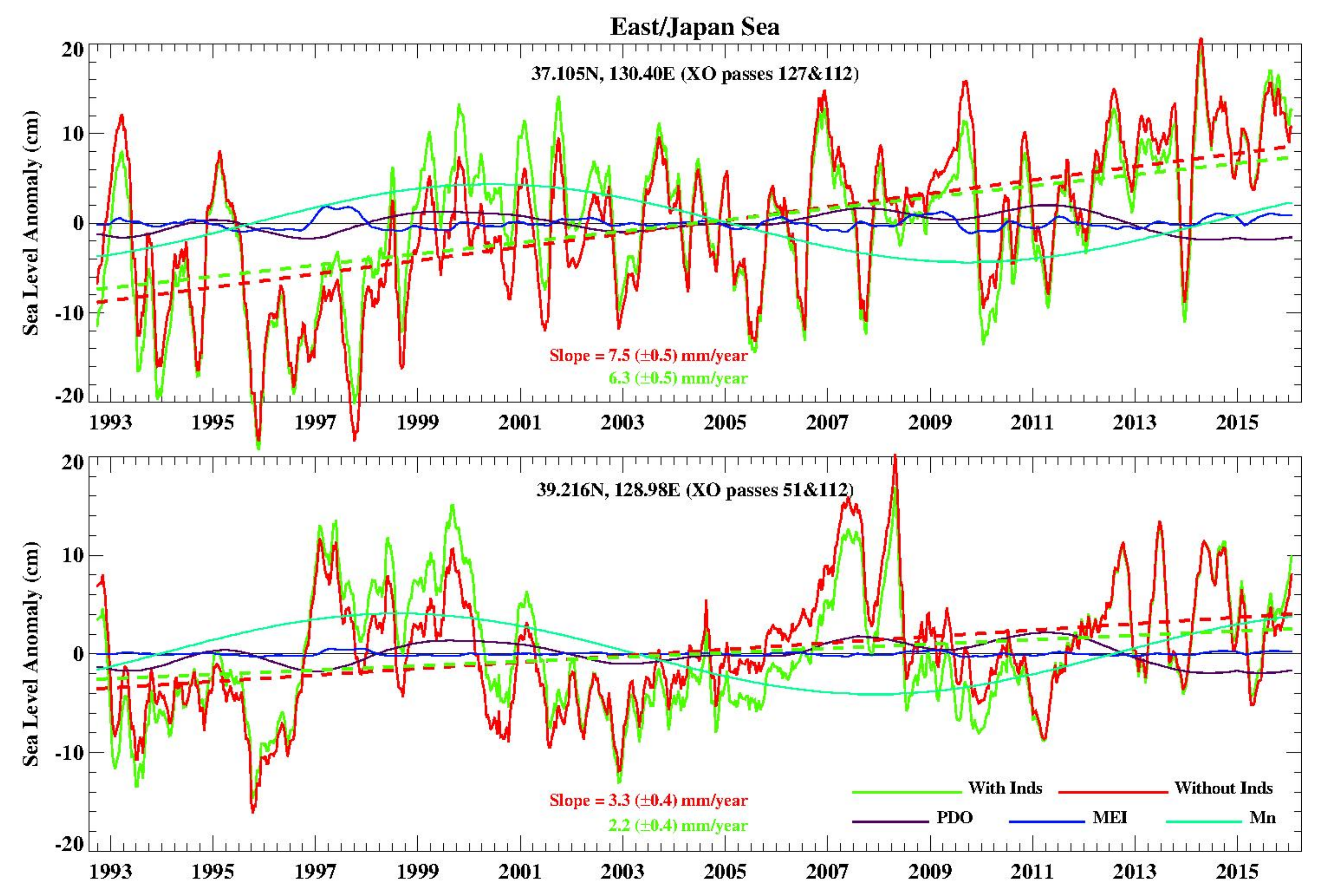
East/Japan Sea
37.105N, 130.40E (XO passes 127&112)
Sea Level Anomaly (cm)
Slope = 7.5 (±0.5) mm/year
6.3 (±0.5) mm/year
39.216N, 128.98E (XO passes 51&112)
Sea Level Anomaly (cm)
Slope = 3.3 (±0.4) mm/year
2.2 (±0.4) mm/year
With Inds
Without Inds
PDO
MEI
Mn
1993
1995
1997
1999
2001
2003
2005
2007
2009
2011
2013
2015

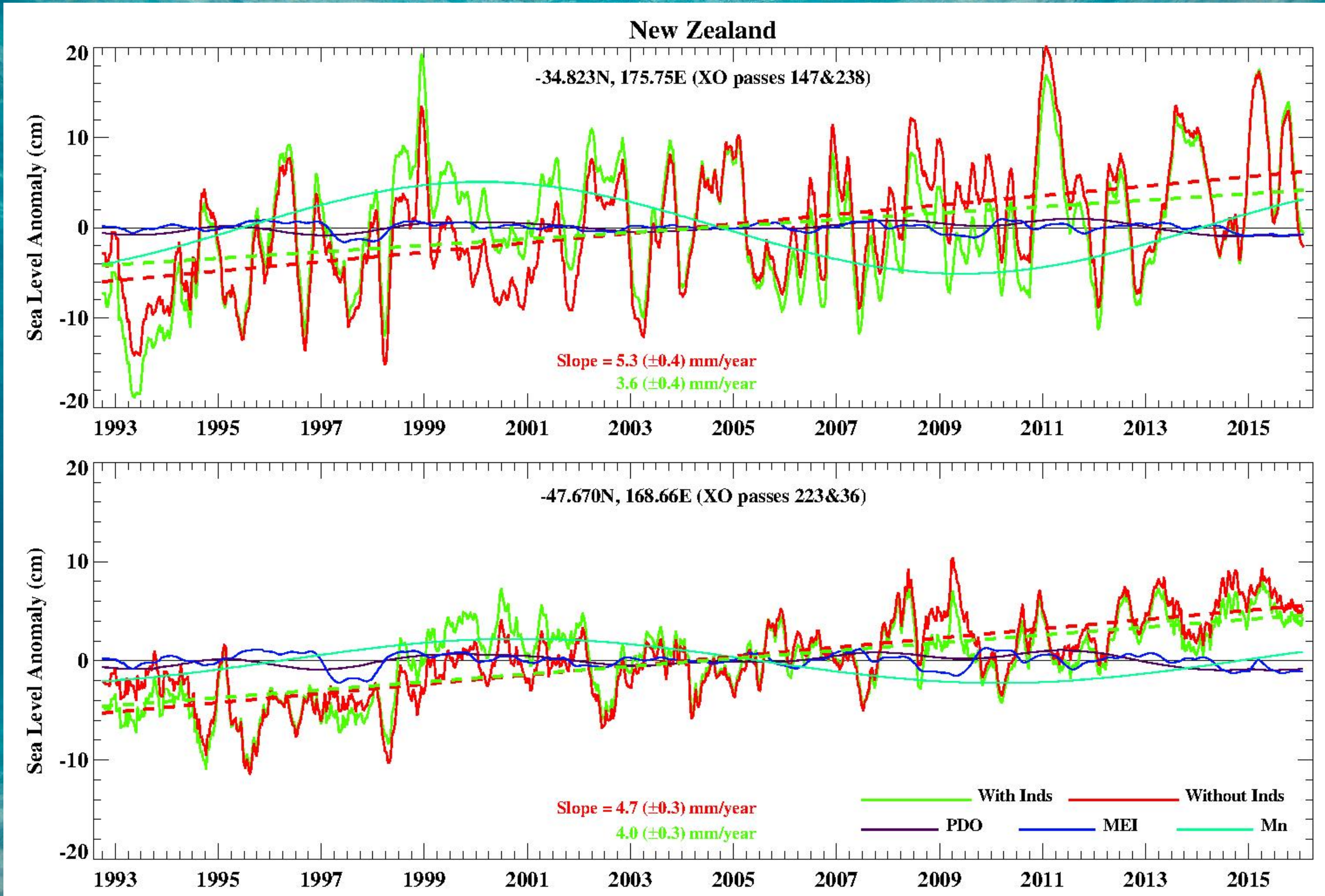
New Zealand
-34.823N, 175.75E (XO passes 147&238)
Sea Level Anomaly (cm)
Slope = 5.3 (±0.4) mm/year
3.6 (±0.4) mm/year
-47.670N, 168.66E (XO passes 223&36)
Slope = 4.7 (±0.3) mm/year
4.0 (±0.3) mm/year
With Inds
Without Inds
PDO
MEI
Mn

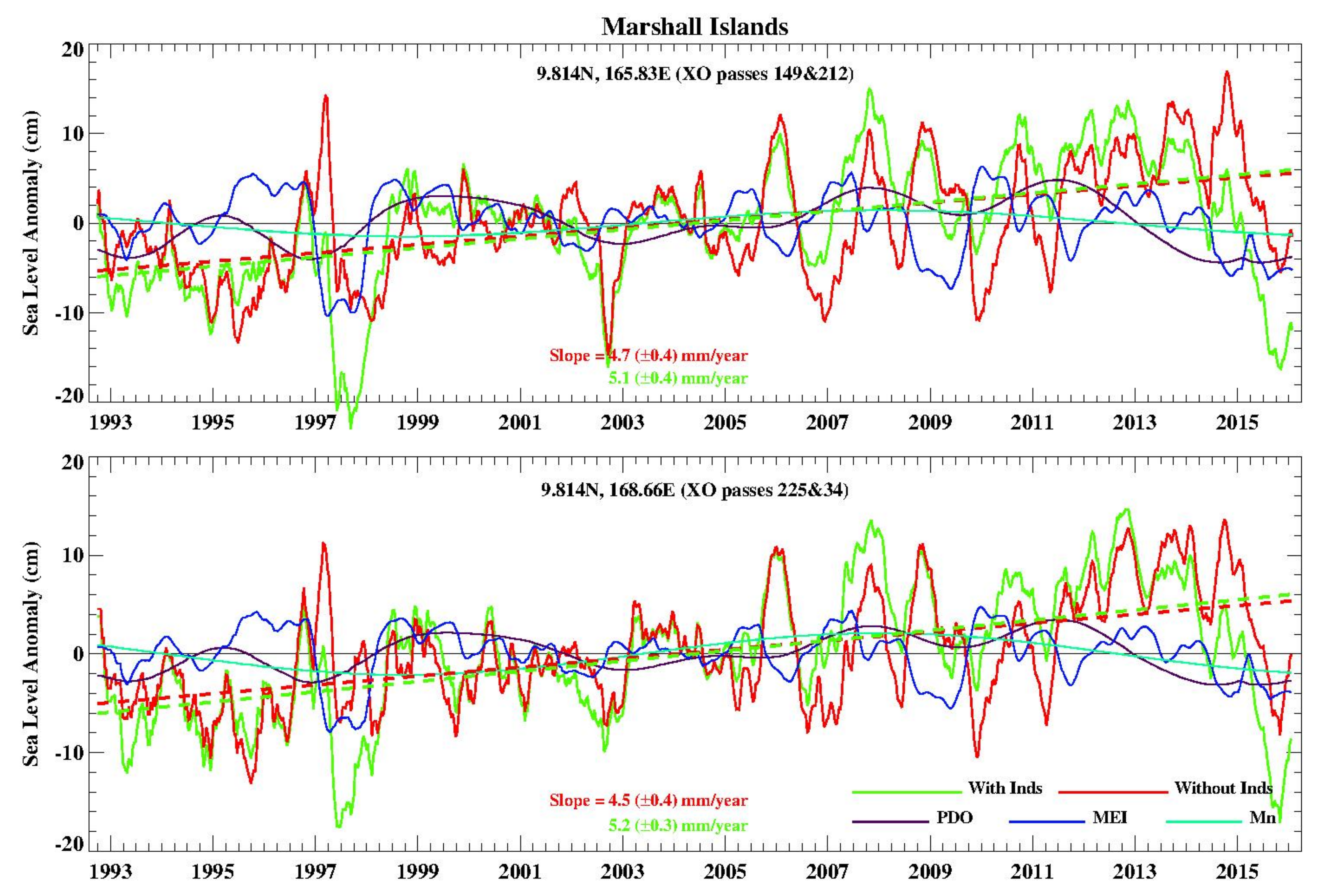

Marshall Islands
9.814N, 165.83E (XO passes 149&212)
Sea Level Anomaly (cm)
Slope = 4.7 (±0.4) mm/year
5.1 (±0.4) mm/year
9.814N, 168.66E (XO passes 225&34)
Slope = 4.5 (±0.4) mm/year
5.2 (±0.3) mm/year
With Inds
Without Inds
PDO
MEI
Mn

TPJ data coverage (%)

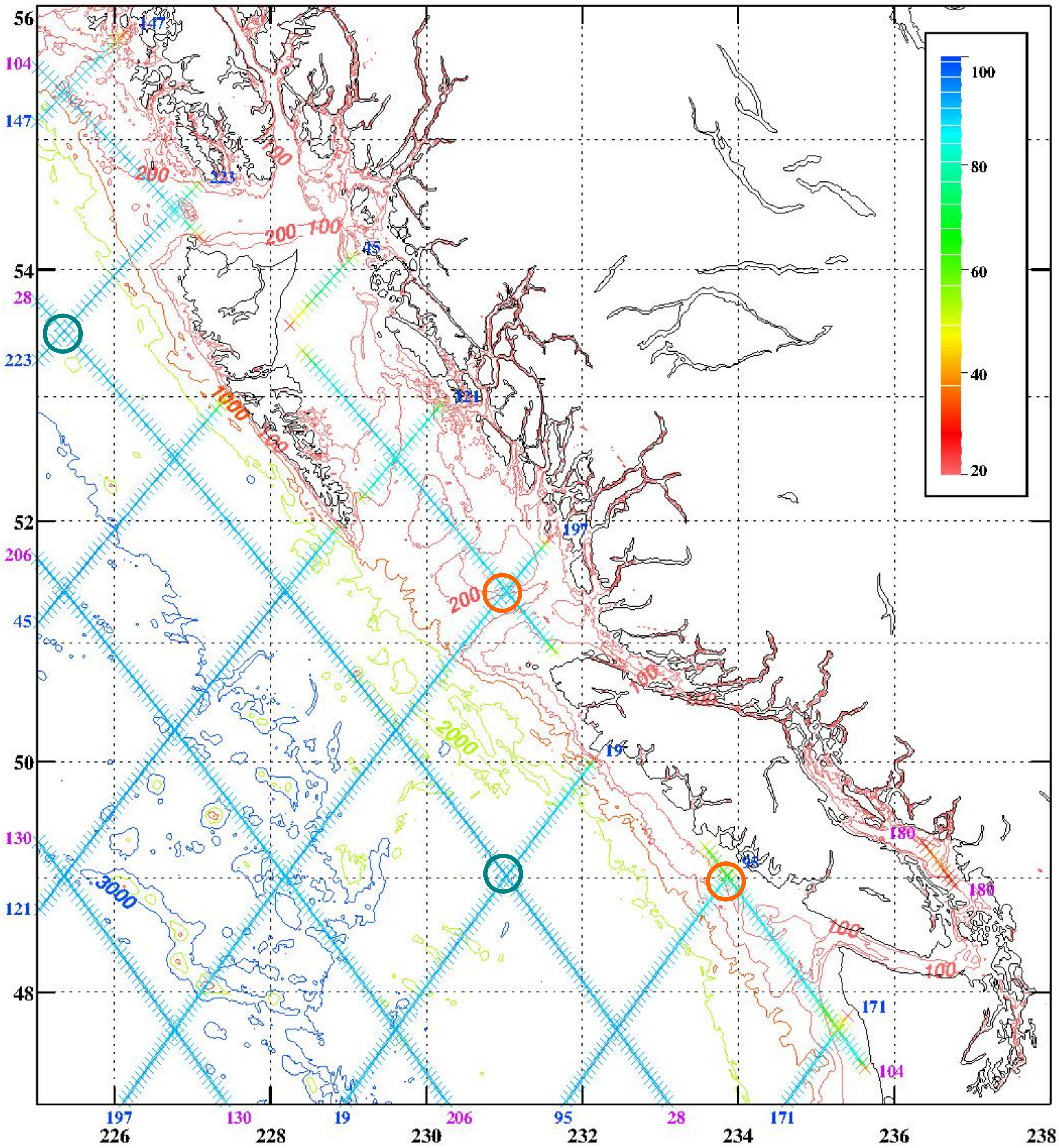

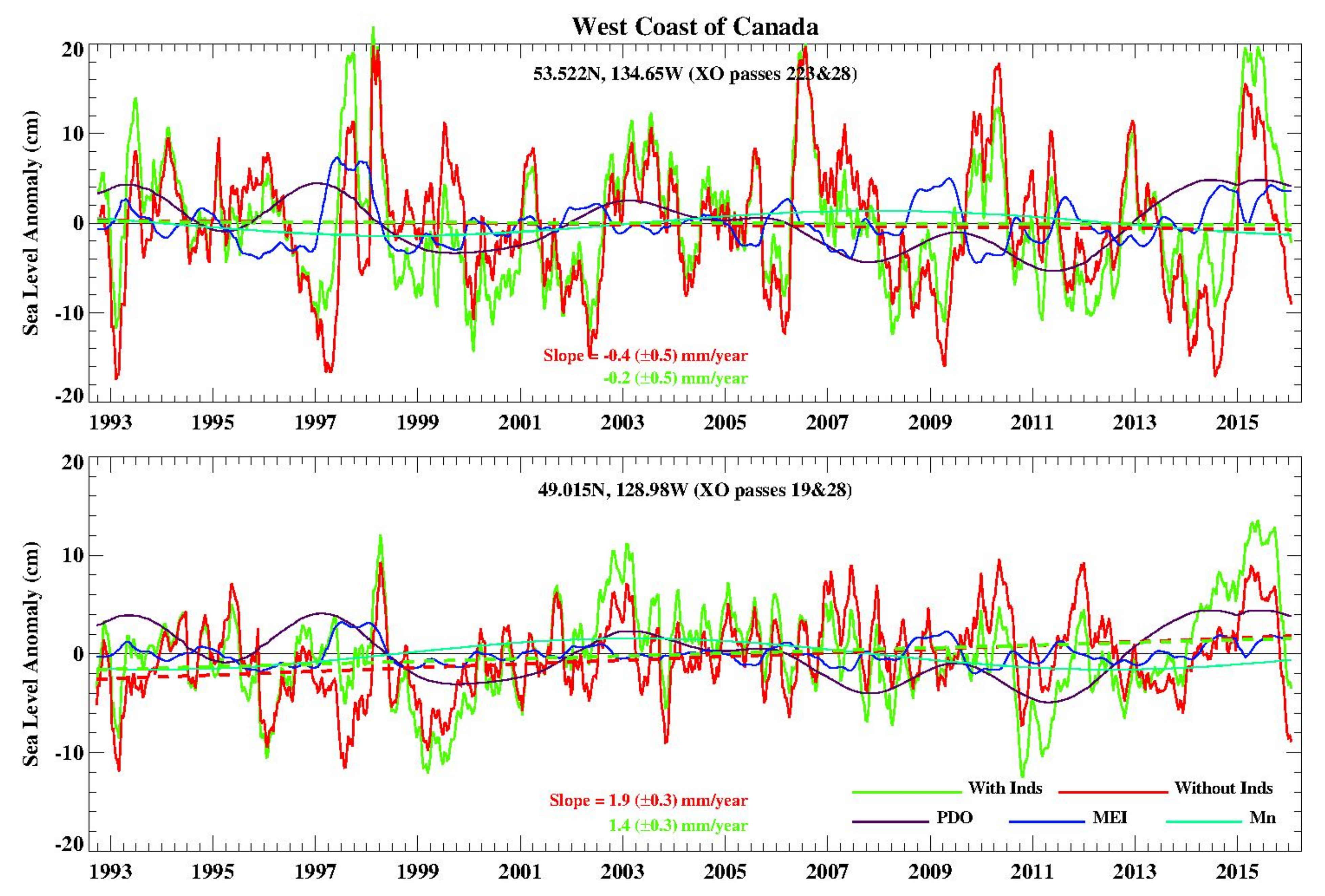
West Coast of Canada
53.522N, 134.65W (XO passes 223&28)
Slope = -0.4 (±0.5) mm/year
-0.2 (±0.5) mm/year
49.015N, 128.98W (XO passes 19&28)
Slope = 1.9 (±0.3) mm/year
1.4 (±0.3) mm/year
Sea Level Anomaly (cm)
With Inds
Without Inds
PDO
MEI
Mn
1993
1995
1997
1999
2001
2003
2005
2007
2009
2011
2013
2015

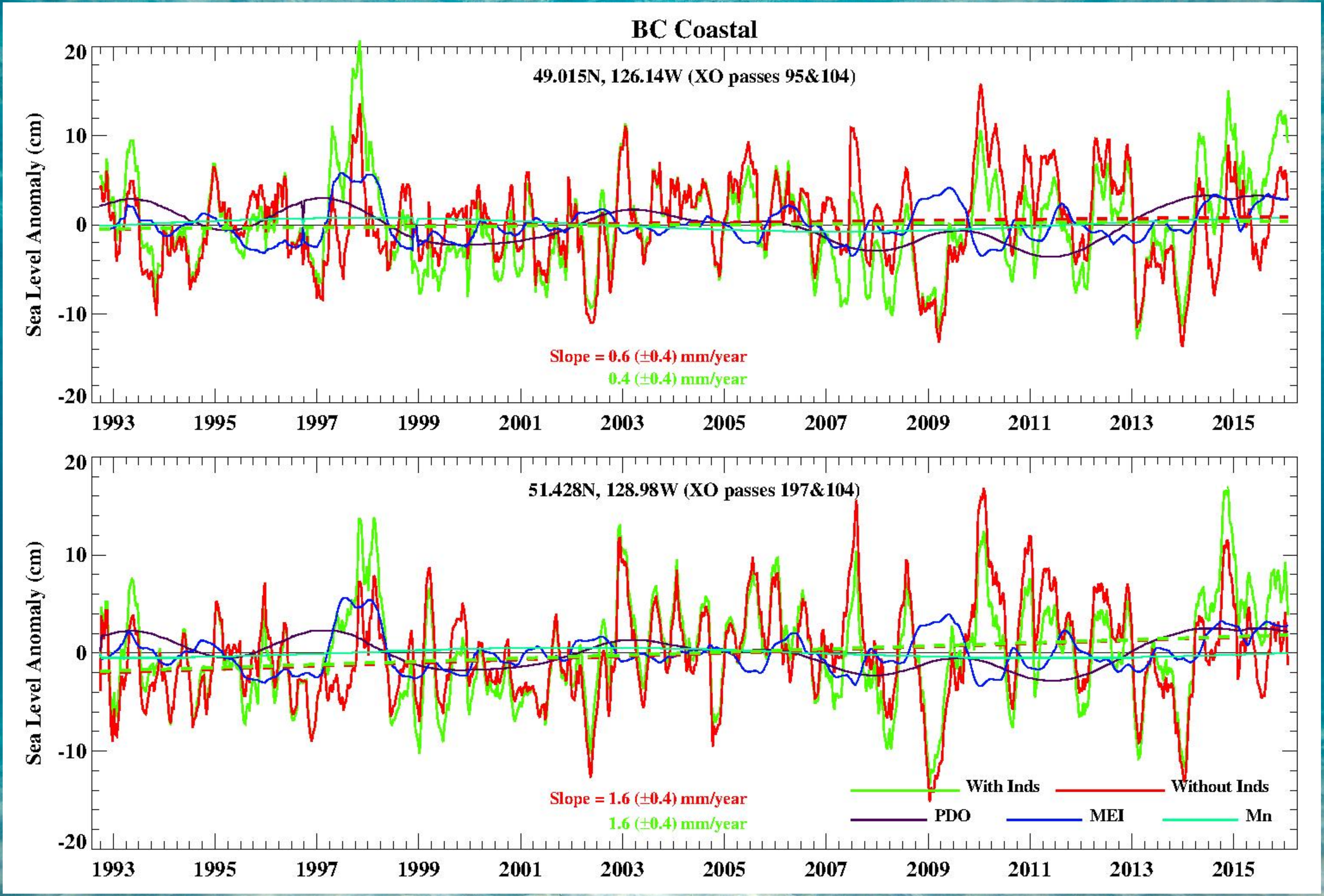
BC Coastal
49.015N, 126.14W (XO passes 95&104)
Sea Level Anomaly (cm)
Slope = 0.6 (±0.4) mm/year
0.4 (±0.4) mm/year
51.428N, 128.98W (XO passes 197&104)
Slope = 1.6 (±0.4) mm/year
1.6 (±0.4) mm/year
With Inds
Without Inds
PDO
MEI
Mn
20
10
0
-10
-20
1993
1995
1997
1999
2001
2003
2005
2007
2009
2011
2013
2015

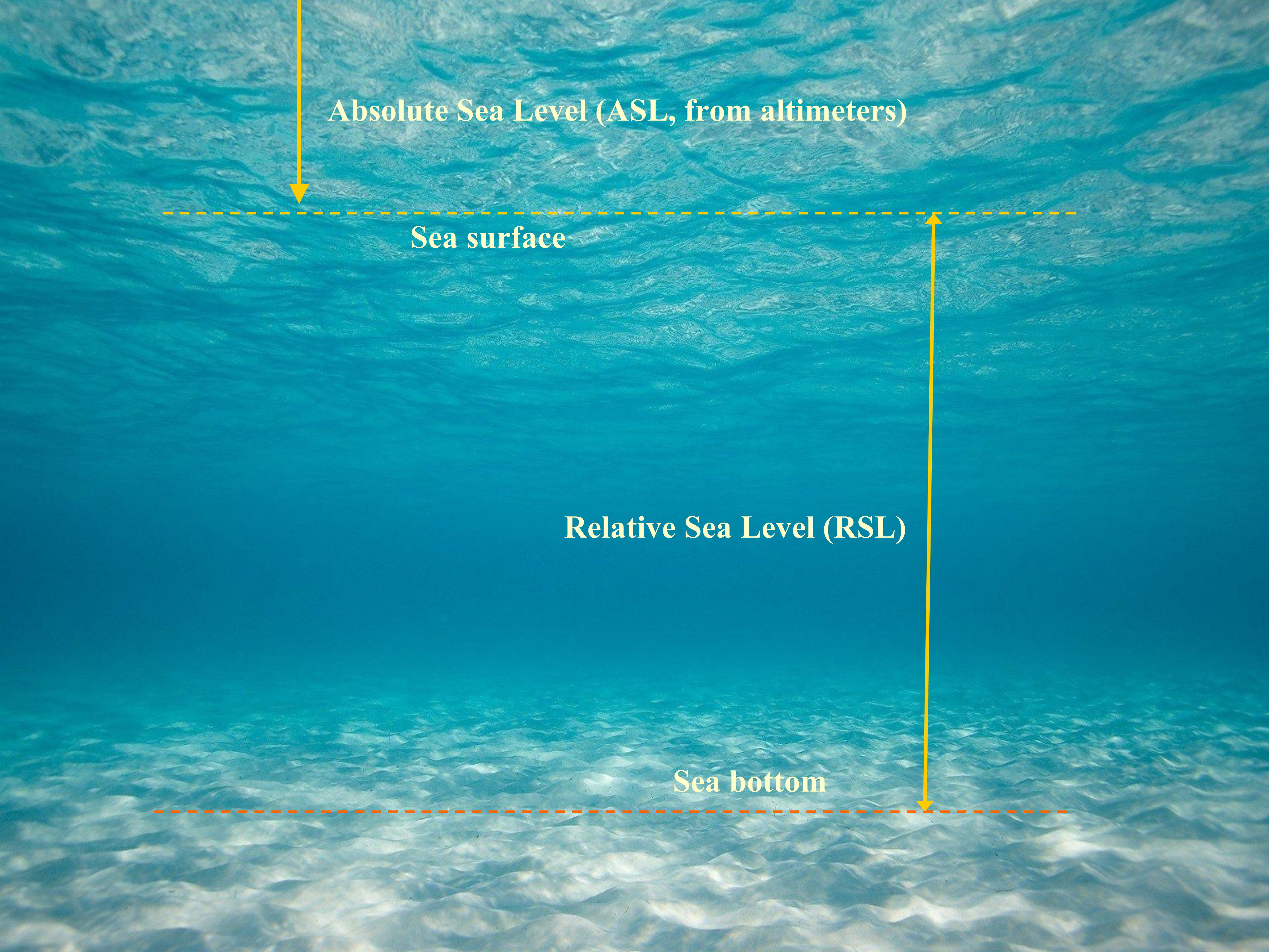
Absolute Sea Level (ASL, from altimeters)
Sea surface
Relative Sea Level (RSL)
Sea bottom

To get RSL from TPJ data, we must add the relative motion of sea bottom (MSB) which may be due to the Glacial Isostatic Adjustment (GIA), tectonic processes (TP), land subsidence (LS)m etc.

However, we do not know the contributions to MSB from these terms well enough, except for GPS data at the coast. We therefore rely on the models.

The following few slides show our initial attempt to include the Peltier et al. (2015) GIA model results in the TPJ altimeter derived sea level trends.

Peltier et al., J. Geophys. Res. (2015): Space geodesy constrains ice age terminal deglaciation: The global ICE-6G_C (VM5a) model.

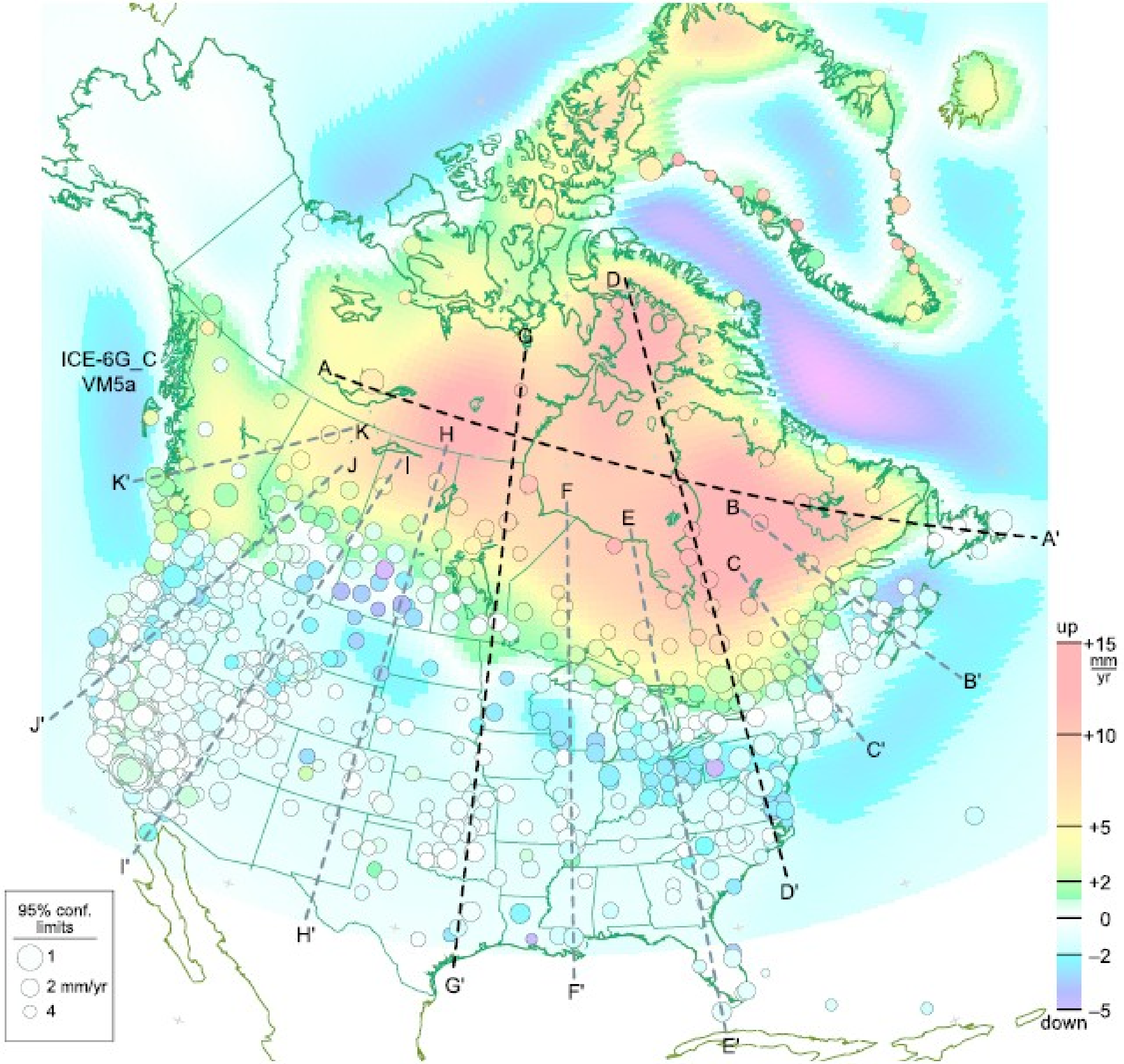

Figure 4. The predicted present-day rate of vertical motion of the crust for the ICE-6G_C (VM5a) model of the global glacial isostatic adjustment process is represented by the background map in which amplitude in mm/yr is represented by the color bar. Superimposed upon this map are the locations of the sites, shown as the open circles, from which GPS measurements of vertical motion are available. The radii of these circles are inversely proportional to the standard error of the individual measurements. Also shown are the traverses along which comparisons are shown in Figures 5a–5c between the predictions of several of the available models including the new model ICE-6G_C (VM5a).

(from Peltier et al., *J. Geophys Res*. 2015)

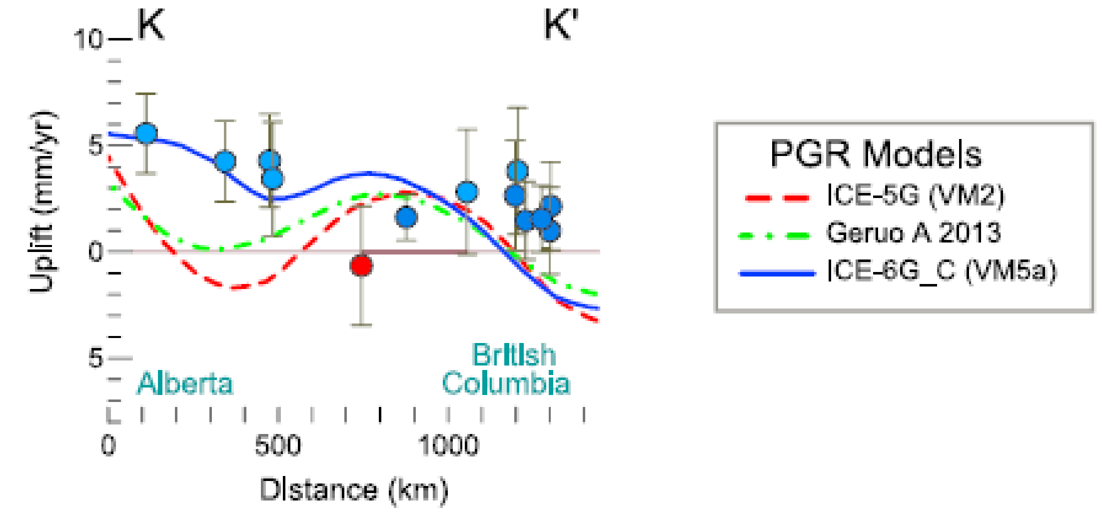

Figure 5. (continued)

Figure 5. (a) Comparisons between GPS observed and GIA model predicted rates of vertical motion along the traverses AA′, DD′, and GG′ shown in Figure 4. Blue sites are from locations that were once ice covered, red sites were never ice covered, and white sites are sufficiently far removed from the line of the traverse that misfits to the data may be ascribable to that source of error. (b) Same as Figure 5a but for the traverses BB′, CC′, EE′, and FF′. (c) Same as Figure 5a but for the traverses HH′–KK′.

(bottom panel of Fig. 5c from Peltier et al., *J. Geophys Res*. 2015)

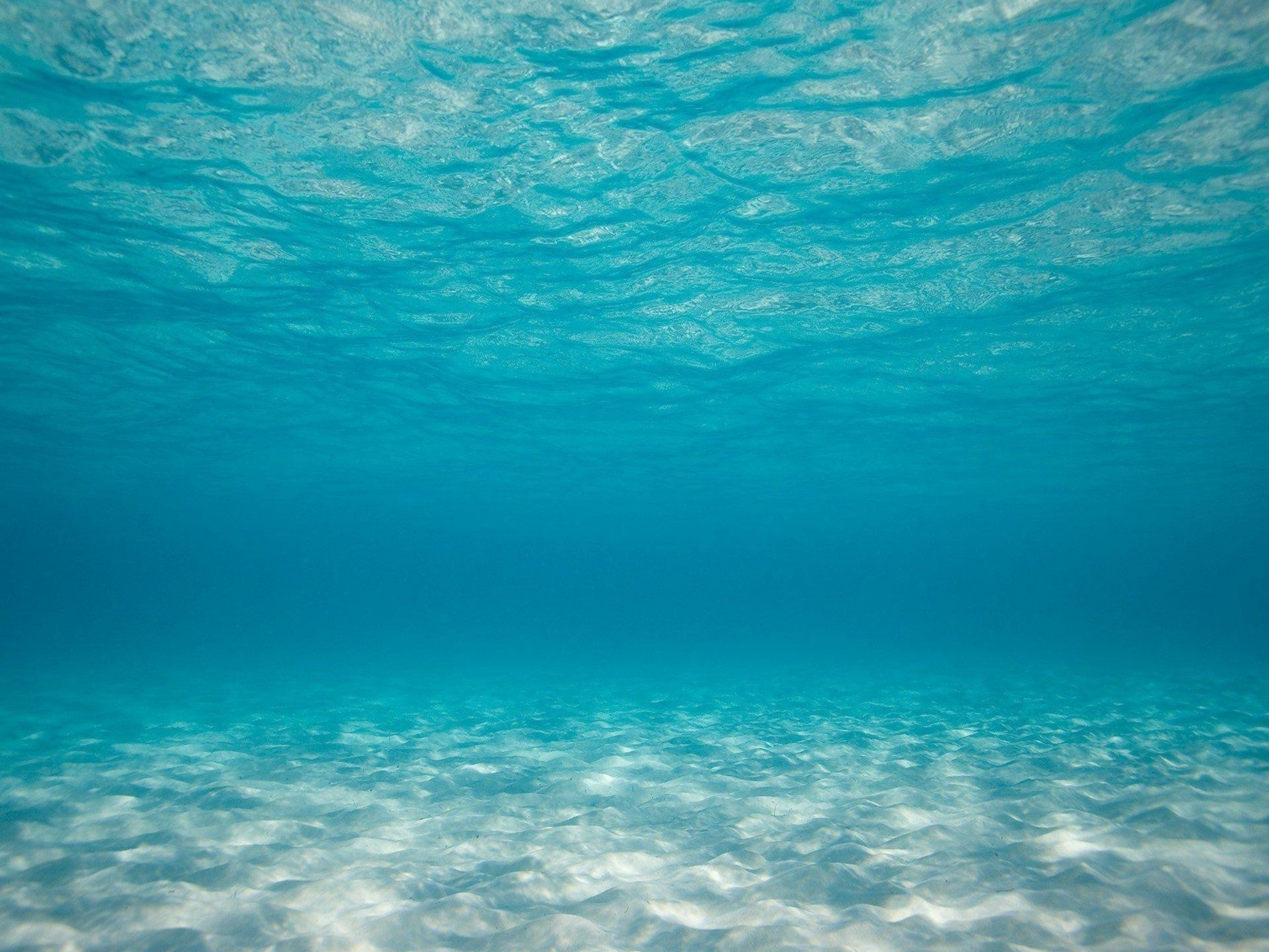

Conclusions

The 23.4-year long TPJ timeseries are now long enough to compute the lunar nodal tide (Mn) and to estimate its contribution to the analyzed Absolute Sea Level (ASL) trends.

Notwithstanding the cross-correlations, it is also useful to include climate index timeseries (such as PDO and MEI) in the Versatile Analysis of sea level observations.

This is quite evident when comparing sea level trends at TPJ cross-overs with and without the contributions from climate indices.

Inclusion of GIA increases the analyzed global mean sea level trend from 2.8 to 3.1 mm/year. However, on smaller regional scales our knowledge of sea bottom motion is not adequate and may lead to erroneous trends.

This further underscores the utmost importance of the coastal tide gauges, which together with ASL from satellite altimeters and data from nearby GPS stations, allow to analyze the Relative Sea Level (RSL) changes at the coast.